

## **Trilliumosides K-L, two novel steroidal saponins from rhizomes of *Trillium govanianum* as potent anticancer agents targeting apoptosis in A-549 cancer cell line.**

**Bashir Ahmad Lone<sup>1,2†</sup>, Misbah Tabassum<sup>1,3†</sup>, Anil Bhushan<sup>1,2</sup>, Dixhya Rani<sup>1,2</sup>, Urvashi Dhiman<sup>1,2</sup>, Ajaz Ahmad<sup>4</sup>, Hilal Ahmad Mir<sup>5</sup>, Prem N. Gupta<sup>1,3</sup>, D. M. Mondhe<sup>1,3</sup>, Sumeet Gairola<sup>1,6</sup> and Prasoon Gupta<sup>1,2\*</sup>**

<sup>1</sup>CSIR-Human Resource Development Centre, Academy of Scientific and Innovative Research, Ghaziabad, India, <sup>2</sup>Natural Products and Medicinal Chemistry Division, CSIR-Indian Institute of Integrative Medicine, Jammu, India, <sup>3</sup>Pharmacology Division, CSIR-Indian Institute of Integrative Medicine, Jammu, India, <sup>4</sup>Department of Clinical Pharmacy, College of Pharmacy, King Saud University, Riyadh 11451, Saudi Arabia, <sup>5</sup>Department of Ophthalmology, Pathology, and Cell Biology, Columbia University, New York, NY, United States, <sup>6</sup>Plant Science and Agrotechnology Division, CSIR-Indian Institute of Integrative Medicine, Jammu, India

### **Abstract**

Two novel steroidal saponins, trilliumosides K (**1**) and L (**2**) were isolated from the rhizomes of *Trillium govanianum* led by bioactivity-guided phytochemical investigation along with seven known compounds govanoside D (**3**) protodioscin (**4**), borassoside E (**5**), 20-hydroxyecdysone (**6**), 5,20-hydroxyecdysone (**7**), govanic acid (**8**) and diosgenin (**9**). The structure of novel compounds 1-2 were established using analysis of spectroscopic data including 1D, 2D NMR and HR-ESI-MS data. All isolated compounds were evaluated for in-vitro cytotoxic activity against a panel of human cancer cell lines. Compound (**1**) showed significant cytotoxic activity against A-549 (Lung) and SW-620 (Colon) cancer cell lines with IC<sub>50</sub> values of 1.83 & 1.85  $\mu$ M, whereas compound (**2**) IC<sub>50</sub> value against A-549 cell line was found to be 1.79  $\mu$ M respectively. Among previously known compounds (**3**), (**5**) and (**9**) their cytotoxic IC<sub>50</sub> value was found to be in the range of 5-10  $\mu$ M. Comprehensive anticancer investigation revealed that compound (**2**) inhibited in-vitro migration and colony forming capability in the A-549 cell line. Additionally, the mechanistic analysis of compound (**2**) on the A-549 cell line indicated distinctive alterations in nuclear morphology, increased reactive oxygen species (ROS) production, and decreased levels of mitochondrial membrane potential (MMP). By upregulating the pro-apoptotic protein BAX and downregulating the anti-apoptotic protein BCL-2, the aforementioned actions eventually cause apoptosis, a

crucial hallmark in cancer research, which activates Caspase-3. To the best of our knowledge, this study reports the first mechanistic anticancer evaluation of the compounds isolated from the rhizomes of *Trillium govanianum* with remarkable cytotoxic activity in the desired micromolar range.

**Keywords:** *Trillium govanianum*, Saponins, Steroidal glycosides, A-549, BAX, BCL-2, cytotoxicity.

**Figure S1.** <sup>1</sup>HNMR spectrum of compound **1** (TG-07 B3) (MeOD<sub>6</sub>, 500 MHz)

**Figure S2.** <sup>13</sup>C NMR spectrum of compound **1** (MeOD<sub>6</sub>, 100 MHz)

**Figure S3.** DEPT spectrum of compound **1** (MeOD<sub>6</sub>, 100 MHz)

**Figure S4.** HSQC spectrum of compound **1**

**Figure S5.** HMBC spectrum of compound **1**

**Figure S6.** COSY spectrum of compound **1**

**Figure S7.** NOESY spectrum of compound **1**

**Figure S8.** ESI-MS spectrum of compound **1**

**Figure S9.** GC/MS analysis of compound **1**

**Figure S10.** <sup>1</sup>HNMR spectrum of compound **2** (TG-09) (MeOD<sub>6</sub>, 500 MHz)

**Figure S11.** <sup>13</sup>C NMR spectrum of compound **2** (CD<sub>3</sub>OD, 500 MHz)

**Figure S12.** DEPT spectrum of compound **2** (CD<sub>3</sub>OD<sub>6</sub>, 500 MHz)

**Figure S13.** HSQC spectrum of compound **2**

**Figure S14.** HMBC spectrum of compound **2**

**Figure S15.** COSY spectrum of compound **2**

**Figure S16.** NOESY spectrum of compound **2**

**Figure S17.** HR-ESIMS spectrum of compound **2**

**Figure S18.** GC/MS analysis of compound **2**

**Figure S19.** <sup>1</sup>HNMR spectrum of compound **3** (TG-12) (CD<sub>3</sub>OD, 500 MHz)

**Figure S20.** <sup>13</sup>C NMR spectrum of compound **3** (CD<sub>3</sub>OD, 100 MHz)

**Figure S21.** <sup>1</sup>HNMR spectrum of compound **4** (TG-04) (CD<sub>3</sub>OD, 500 MHz)

**Figure S22.** <sup>13</sup>C NMR spectrum of compound **4** (CD<sub>3</sub>OD, 100 MHz)

**Figure S23.** <sup>1</sup>HNMR spectrum of compound **5** (TG-08) (CD<sub>3</sub>OD, 500 MHz)

**Figure S24.**  $^{13}\text{C}$  NMR spectrum of compound **5** ( $\text{CD}_3\text{OD}$ , 100 MHz)

**Figure S25.**  $^1\text{H}$ NMR spectrum of compound **6 (TG-01)** ( $\text{CD}_3\text{OD}$ , 500 MHz)

**Figure S26.**  $^{13}\text{C}$  NMR spectrum of compound **6** ( $\text{CD}_3\text{OD}$ , 100 MHz)

**Figure S27.**  $^1\text{H}$ NMR spectrum of compound **7 (TG-02)** ( $\text{CDCl}_3$ , 500 MHz)

**Figure S28.**  $^{13}\text{C}$  NMR spectrum of compound **7** ( $\text{CDCl}_3$ , 100 MHz)

**Figure S29.**  $^1\text{H}$ NMR spectrum of compound **8 (TG-05)** ( $\text{CD}_3\text{OD}$ , 500 MHz)

**Figure S30.**  $^{13}\text{C}$  NMR spectrum of compound **8** ( $\text{MeOD}_6$ , 100 MHz)

**Figure S31.**  $^1\text{H}$ NMR spectrum of compound **9 (TG-06)** ( $\text{CD}_3\text{OD}$ , 500 MHz)

**Figure S32.**  $^{13}\text{C}$  NMR spectrum of compound **9** ( $\text{CD}_3\text{OD}$ , 100 MHz)

**Table 1 S33.** Growth inhibitory effect of Extracts and enriched fractions

**Table 2 S34.** SRB assay-based screening results.

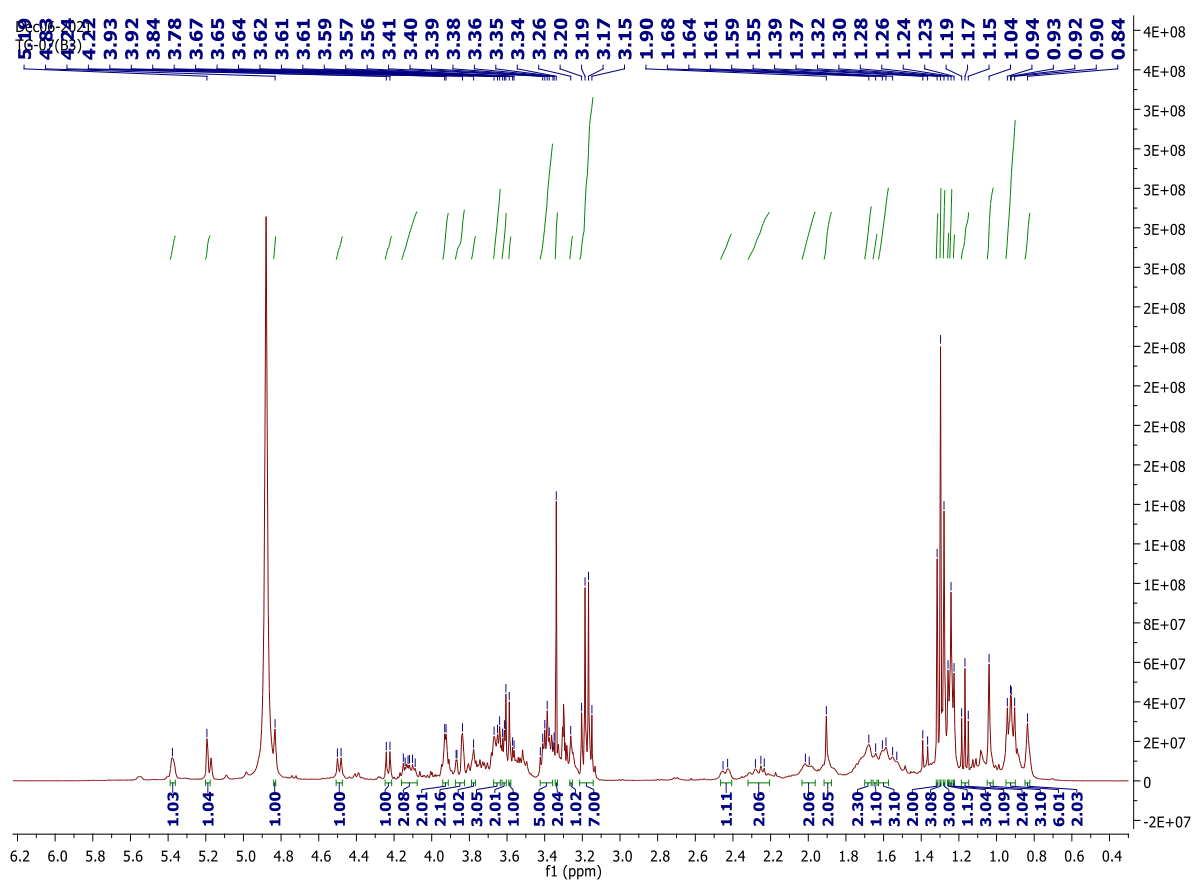


**Figure S1.**  $^1\text{H}$  NMR (400 MHz,  $\text{CD}_3\text{OD}$ ) of compound TG 07 B3

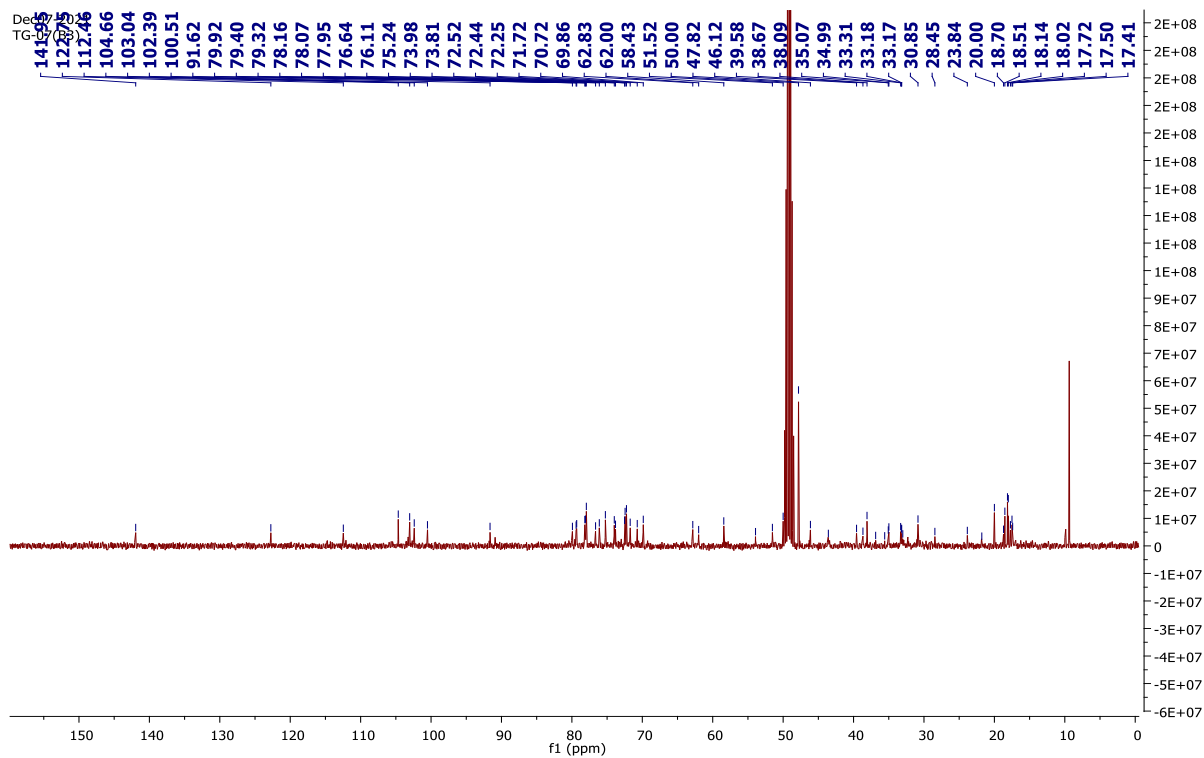


**Figure S2.**  $^{13}\text{C}$  NMR (400 MHz,  $\text{CD}_3\text{OD}$ ) of compound TG 07 B3

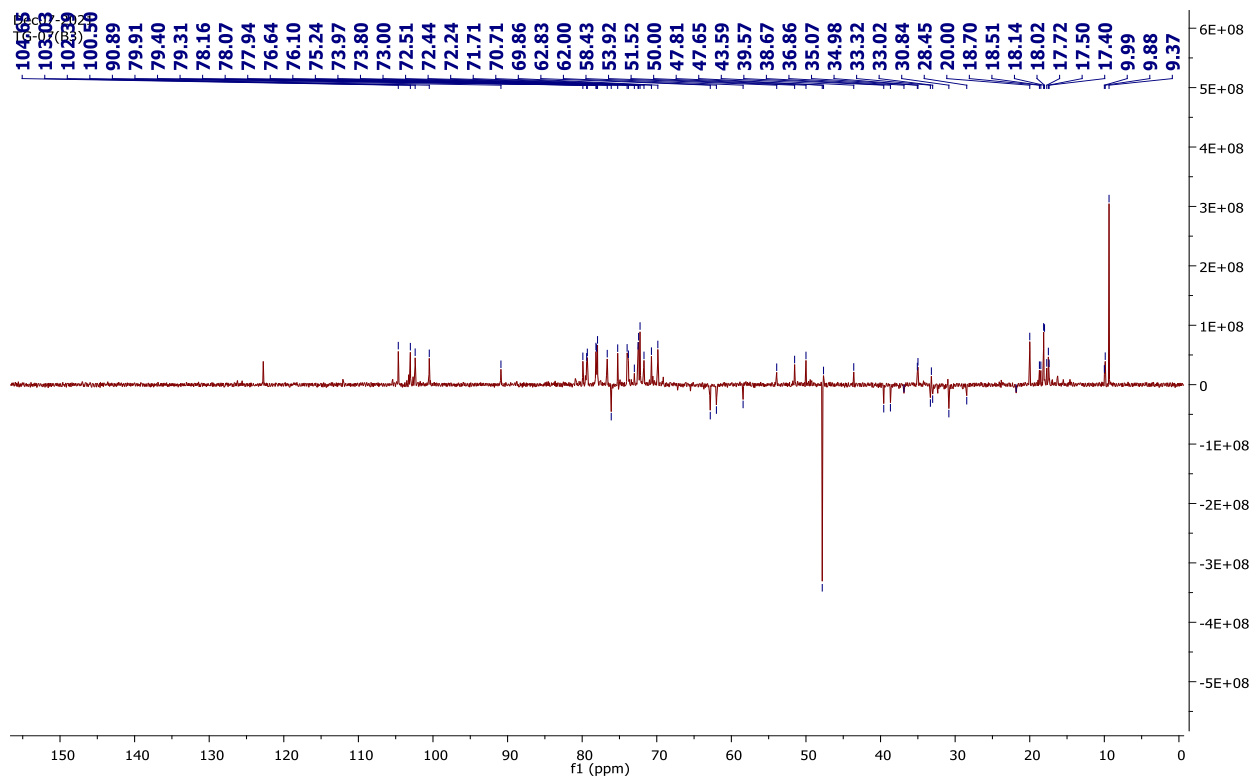


**Figure S3.** DEPT Spectra of compound TG 07 B3

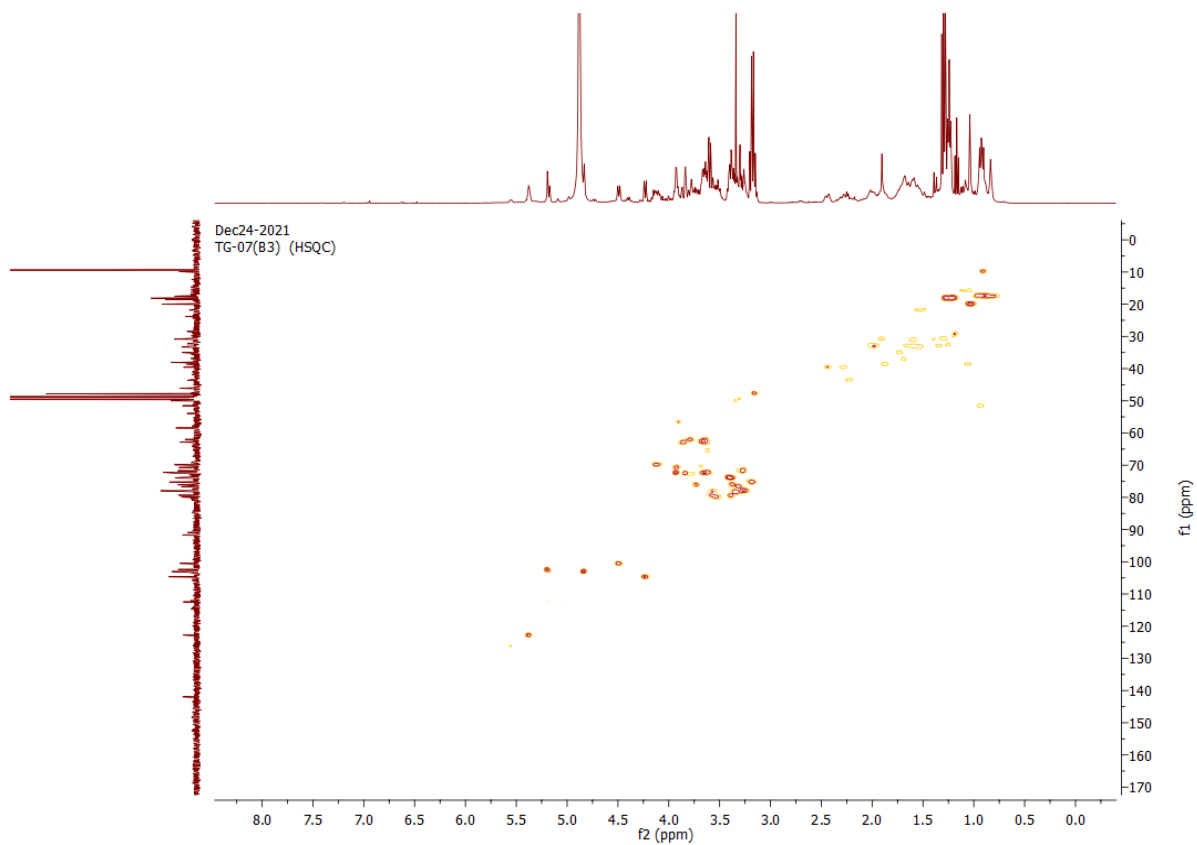


**Figure S4.** HSQC Spectra of compound TG 07 B3

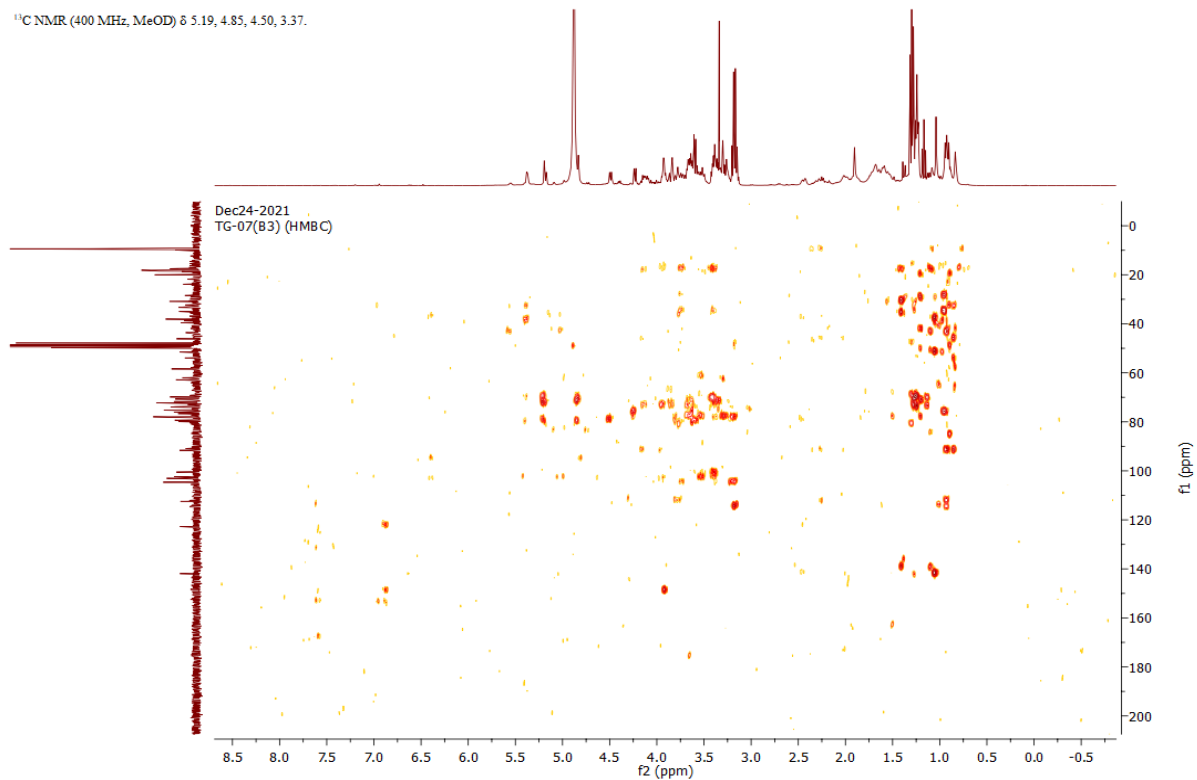


**Figure S5.** HMBC Spectra of compound TG 07 B3

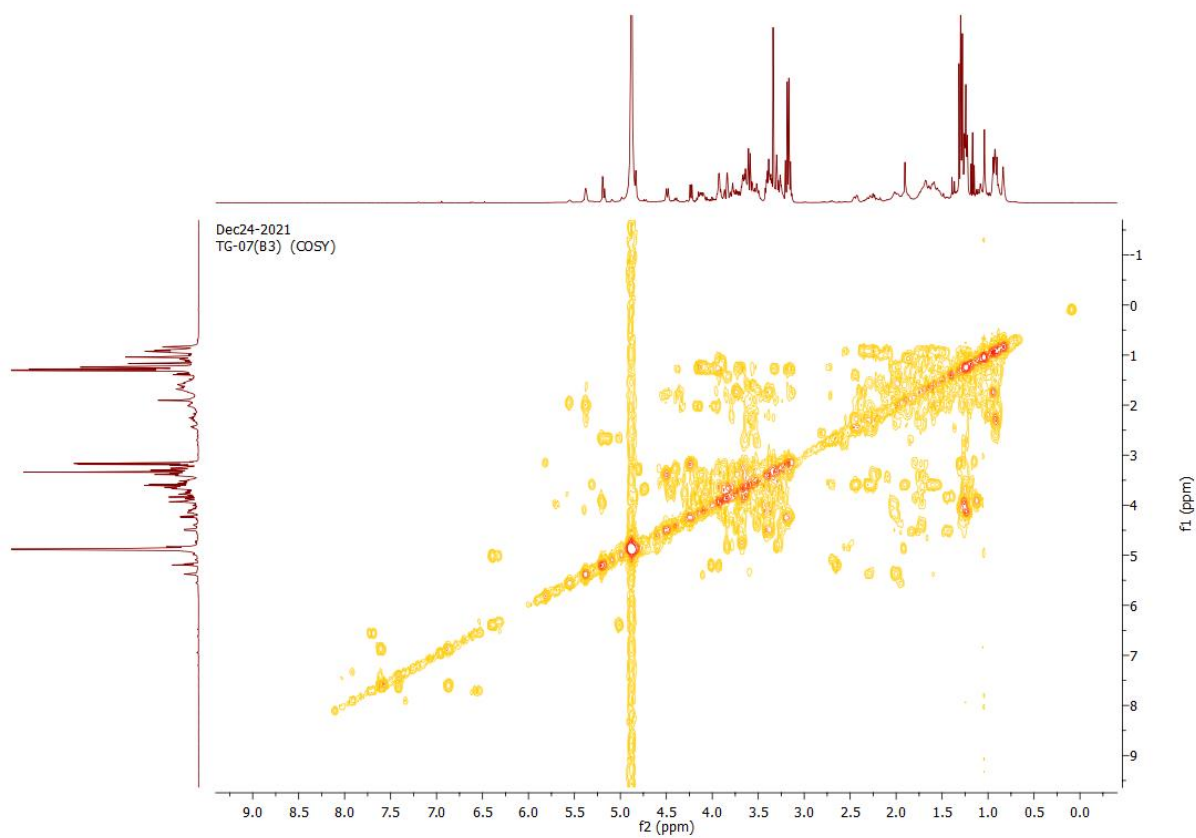


**Figure S6.** COSY Spectra of compound TG 07 B3

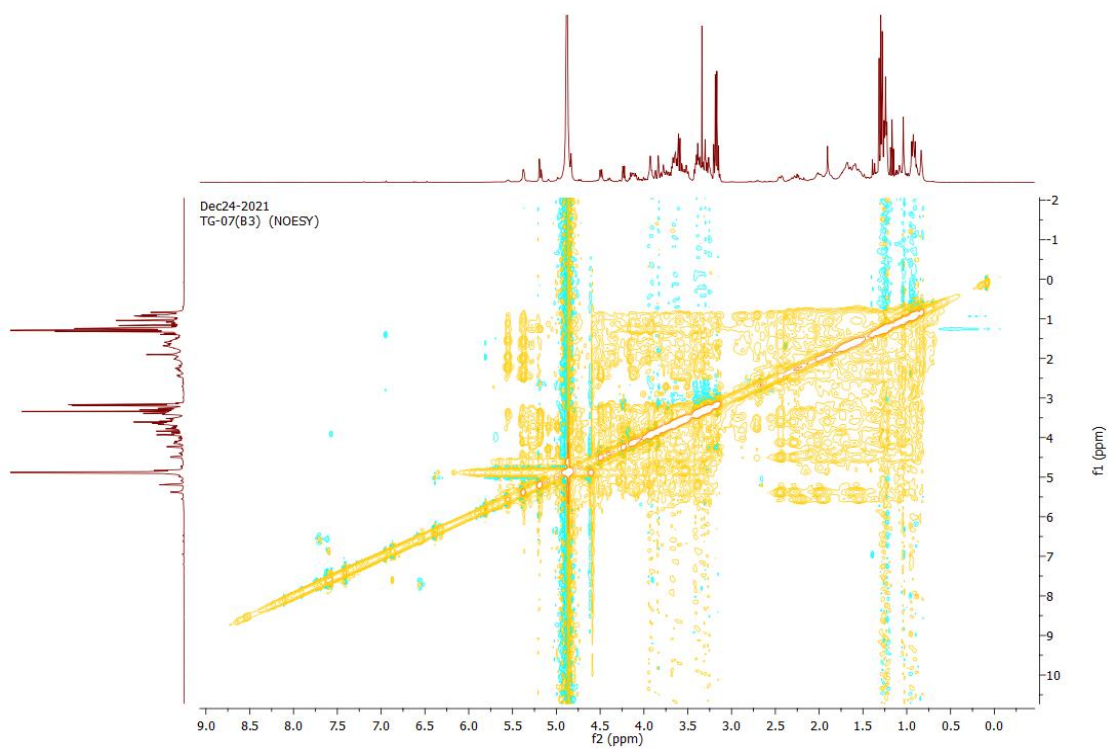


**Figure S7.** NOESY Spectra of compound TG 07 B3

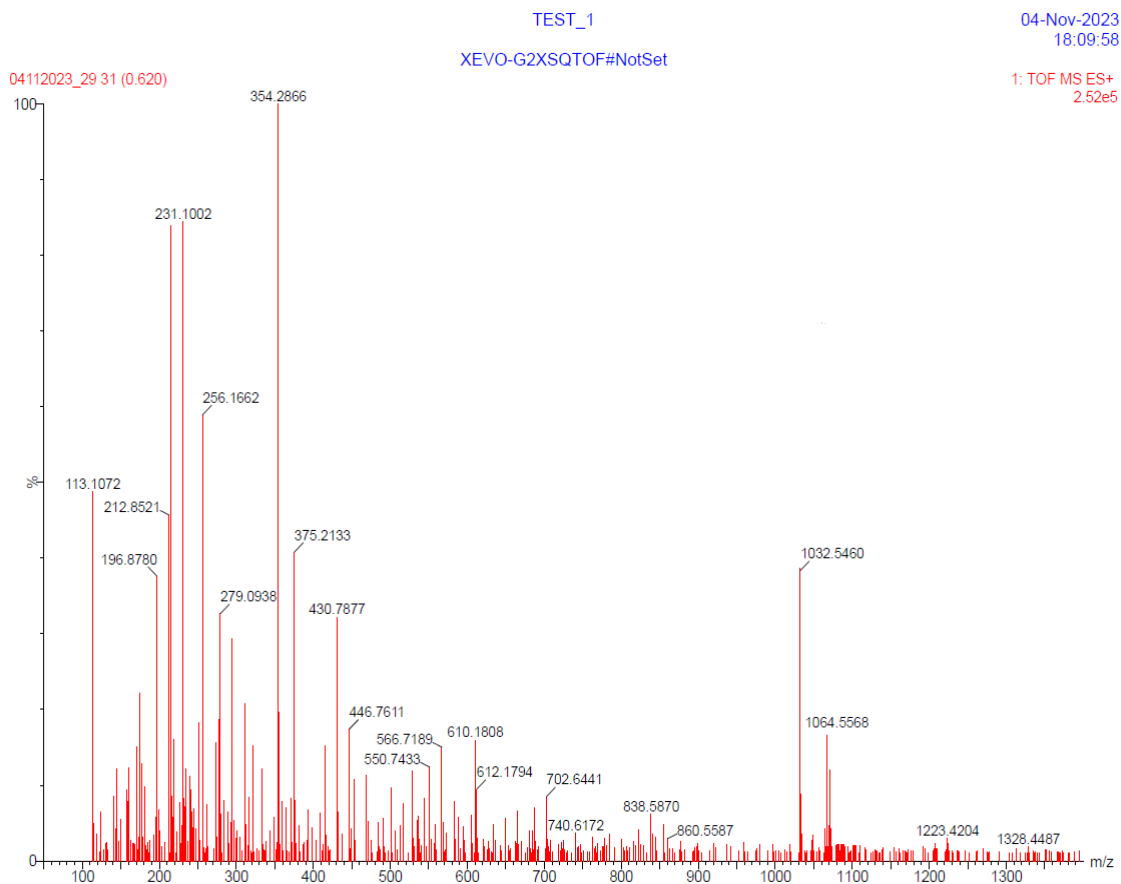


**Figure S8A.** LC/MS of Compound 1

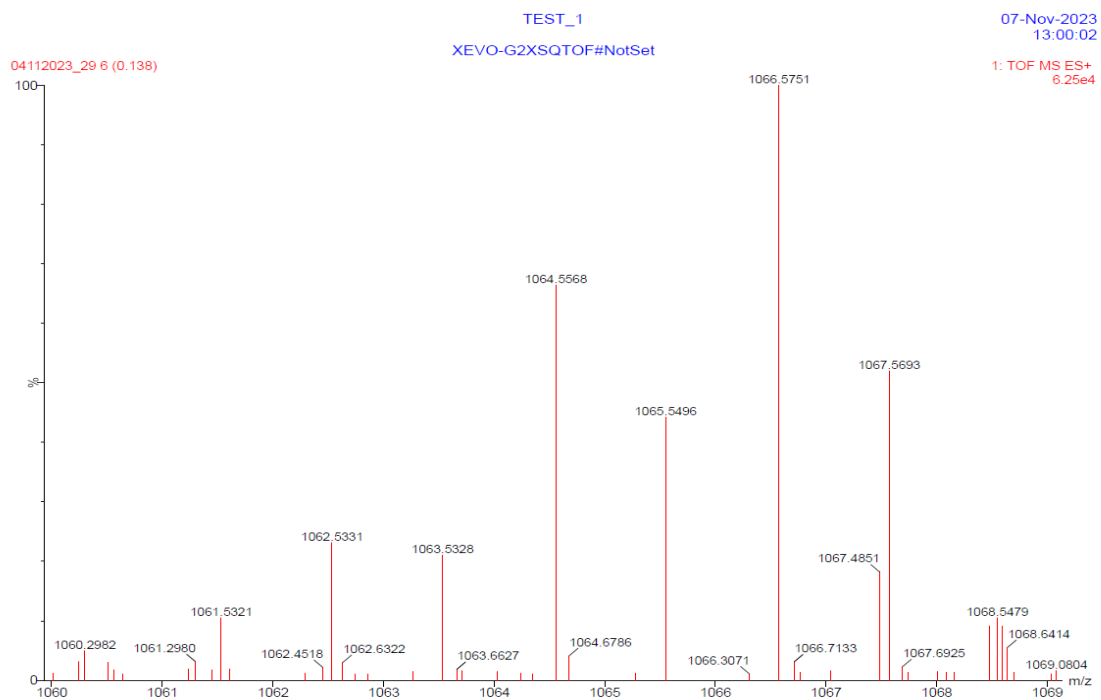
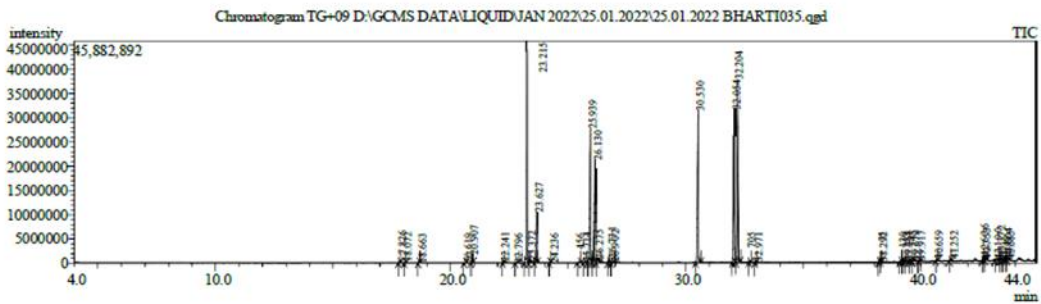


**Figure S8B.** LC/MS of Compound 1.

# IIM GCMS ANALYSIS REPORT

**Sample Information**

Analyzed by : ADMIN  
 Analyzed : 1/27/2022 12:05:44 AM  
 Sample Type : Unknown  
 Sample Name : TG+09  
 Sample Amount : 1  
 Vial # : 4  
 Injection Volume : 0.50  
 Data File : D:\GCMS DATA\LIQUID\JAN 2022\25.01.2022\25.01.2022 BHARTI035.qgd  
 Method File : D:\GCMS METHOD\GCMS-GENERAL\AMIT 1.qgm  
 Tuning File : D:\Tuning\Tuning-NM-F1 18.01.2022.qgt  
 Modified by : Admin  
 Modified : 1/27/2022 12:50:36 AM



Peak#	R.Time	Area	Area%	Height	Similarity	Name
1	23.215	111246953	6.60	45790083	93	Acetyl 2,3,4-tri-O-acetyl-6-deoxy- $\alpha$ -D-glucopyranosid
2	23.627	26047880	1.89	10498744	96	$\alpha$ -1-Talopyranoside, methyl 6-deoxy-, triacetate
3	25.939	99084960	14.79	27692680	95	Acetyl 2,3,4-tri-O-acetyl-6-deoxy- $\alpha$ -D-glucopyranoside
4	26.130	73864469	11.02	21246385	92	115.05 Tetraacetyl- $\beta$ -D-rhamnose
5	30.530	113234727	16.90	31488565	97	Methyl 2,3,4,6-tetra-O-acetyl- $\beta$ -D-glucopyranoside
6	32.054	915066032	23.66	31798909	94	$\beta$ -D-Galactopyranose, pentaacetate
7	32.204	110910512	16.55	37520918	93	$\beta$ -D-Glucopyranose pentaacetate

**Figure S9.** GC/MS analysis of compound 1 (TG 07 B3)

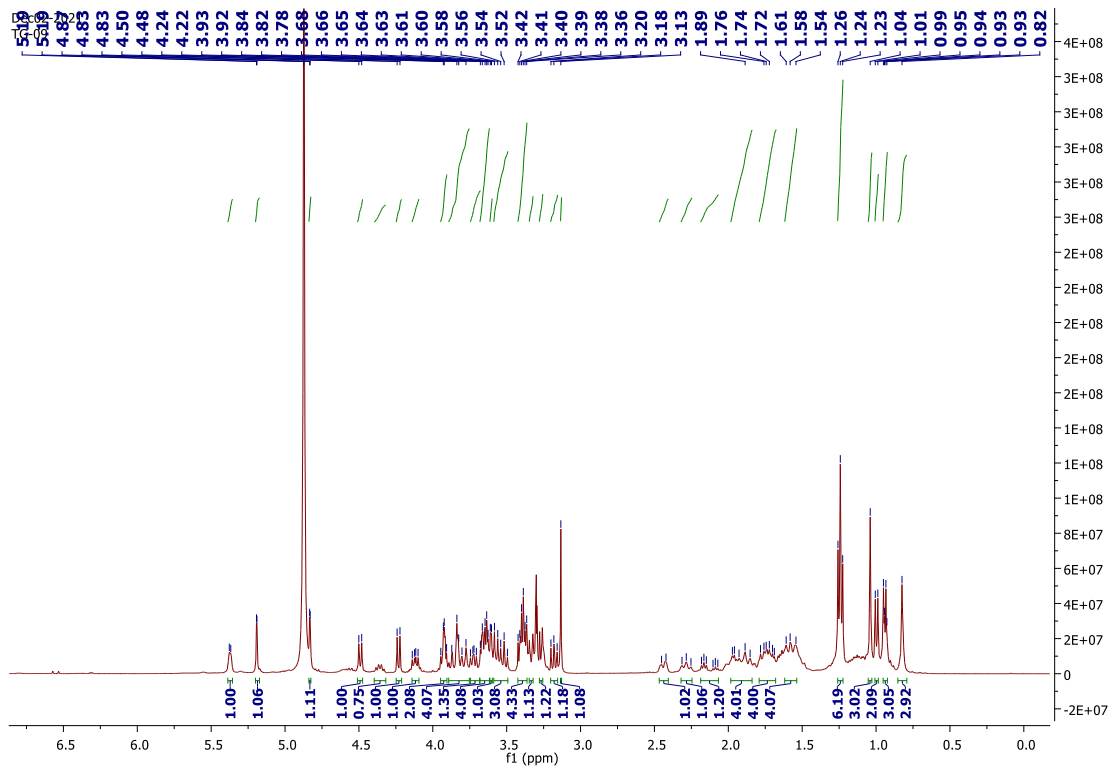




**Figure S10.**  $^1\text{H}$  NMR (400 MHz,  $\text{CD}_3\text{OD}$ ) of compound TG 09

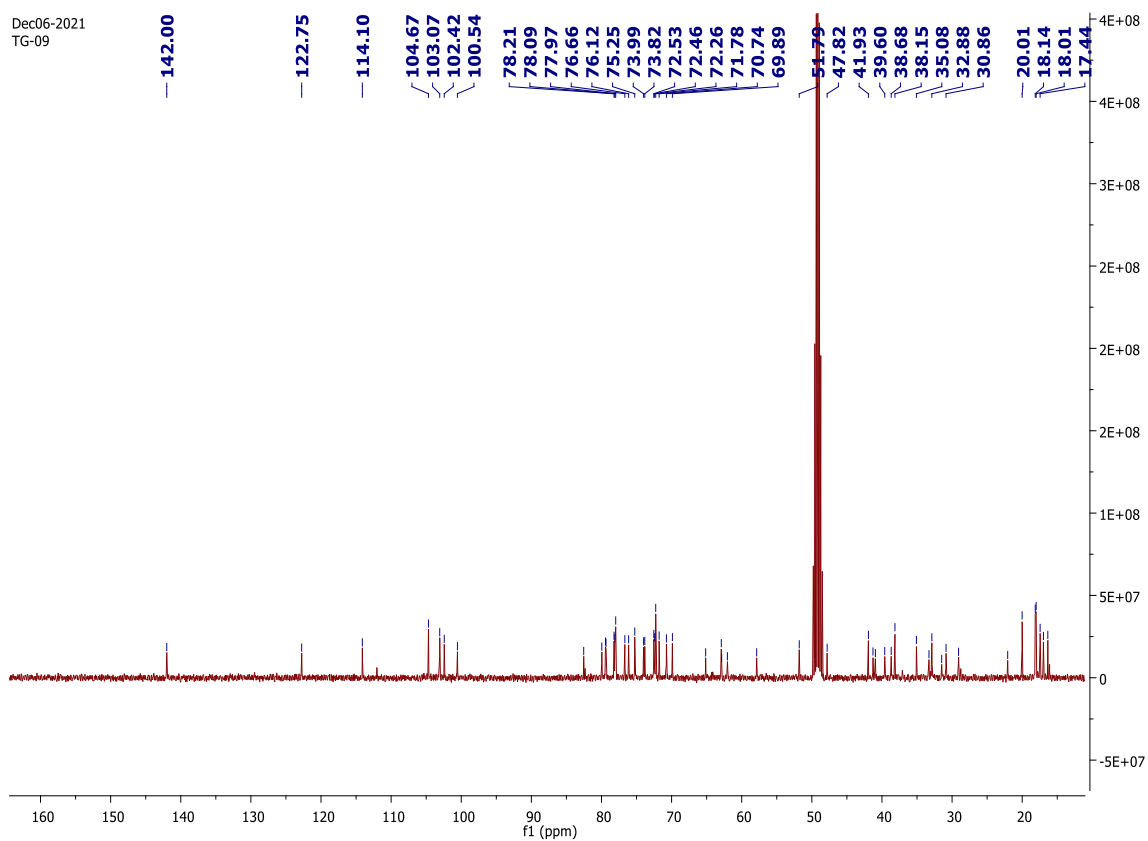


**Figure S11.**  $^{13}\text{C}$  NMR (400 MHz,  $\text{CD}_3\text{OD}$ ) of compound TG 09

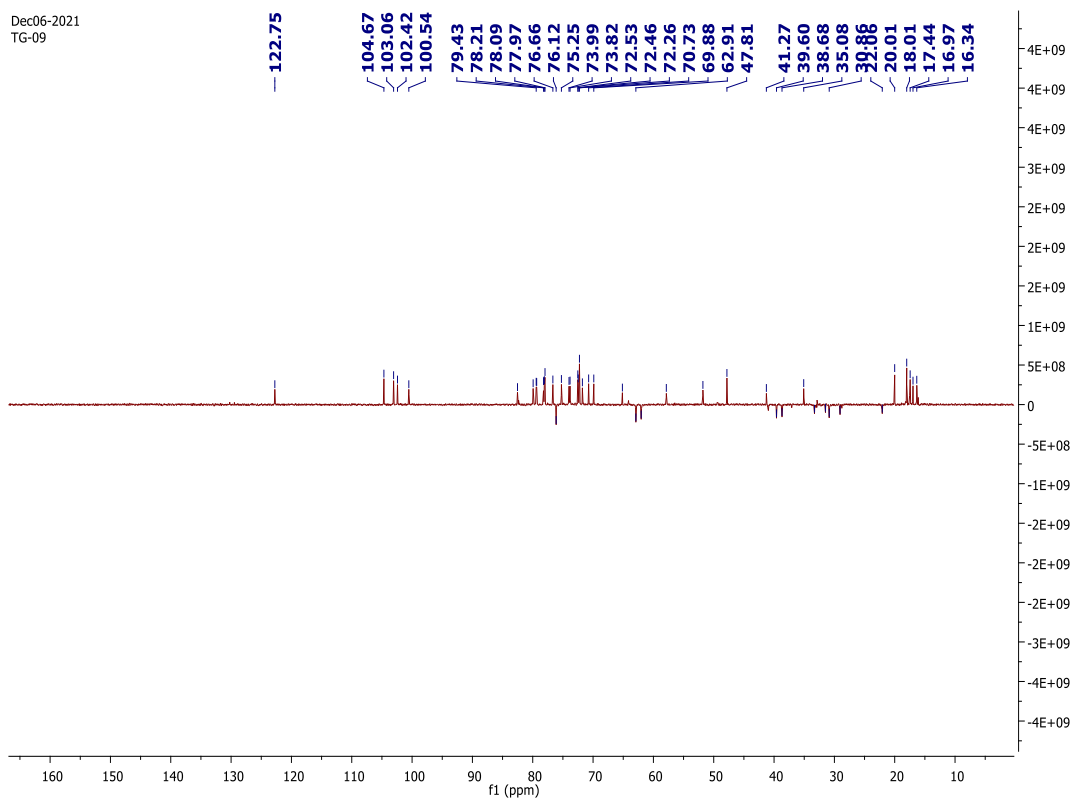


**Figure S12.** DEPT Spectra of compound TG 09

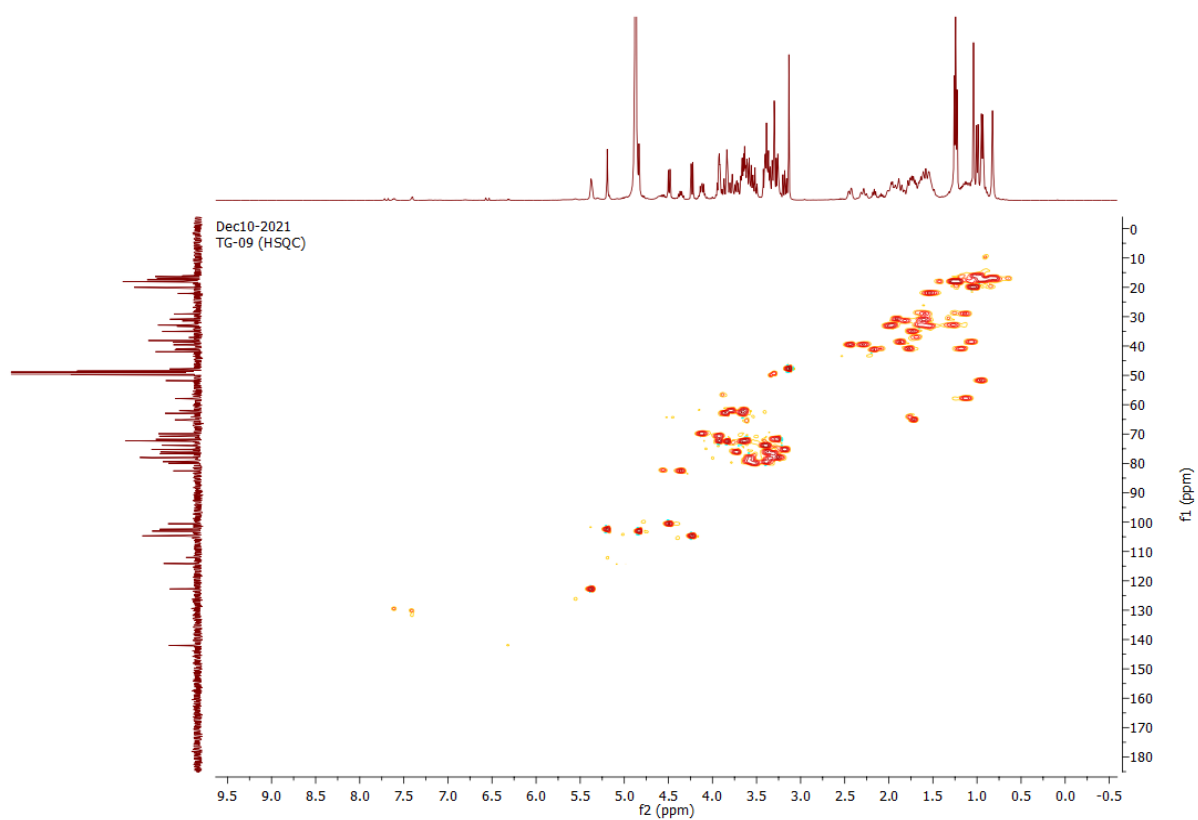


**Figure S13.** HSQC Spectra of compound TG 09

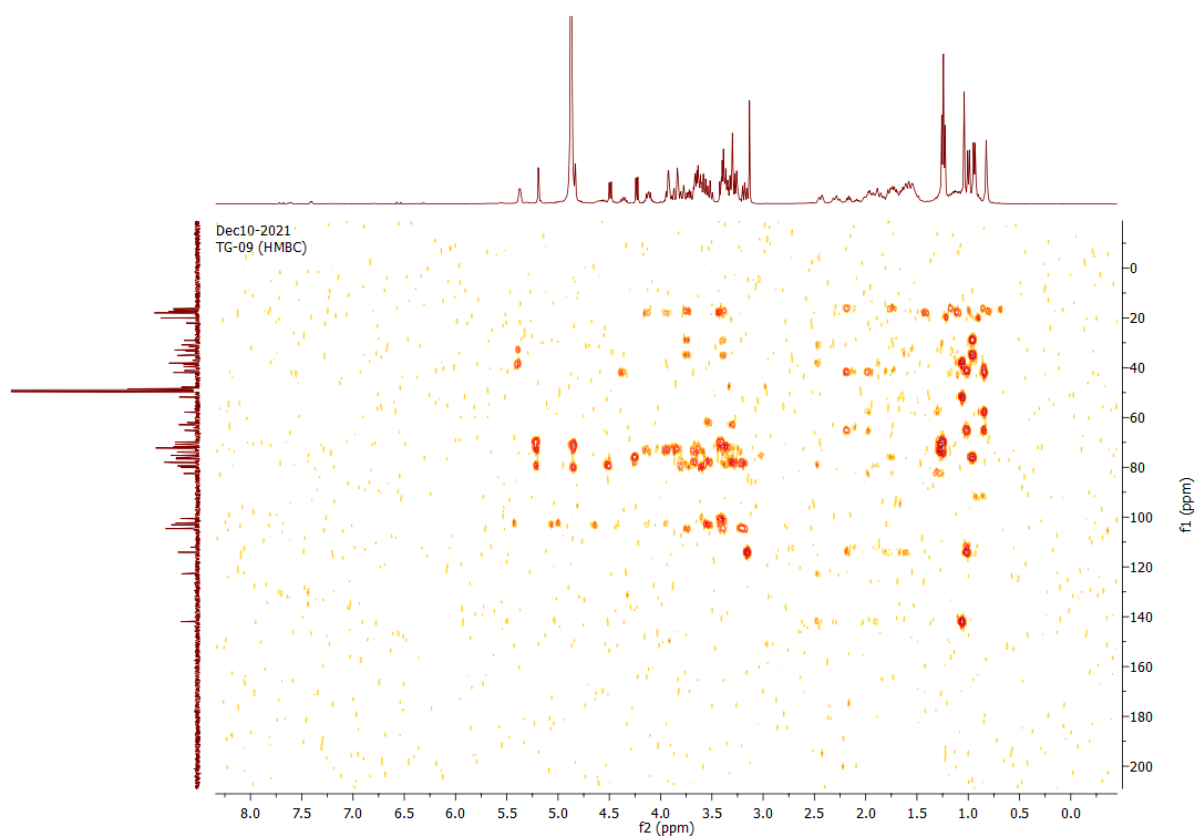


**Figure S14.** HMBC Spectra of compound TG 09

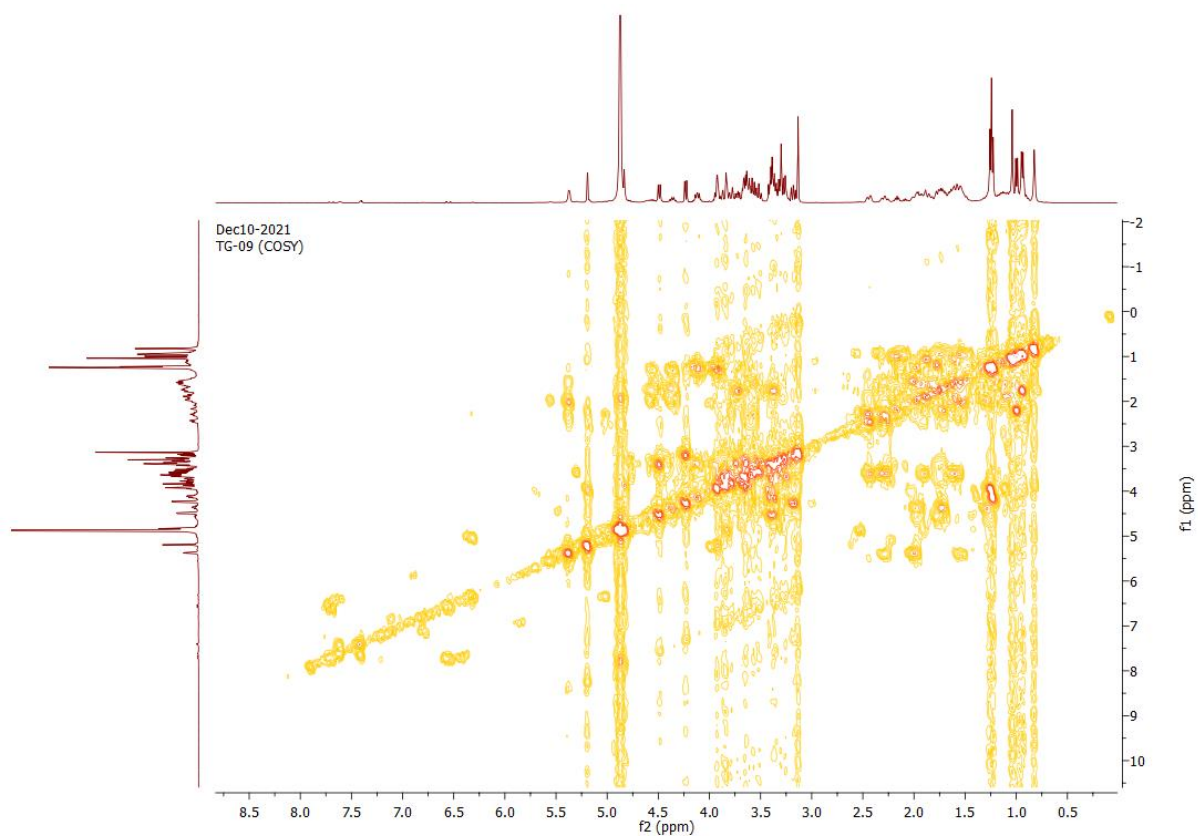


**Figure S15.** COSY Spectra of compound TG 09

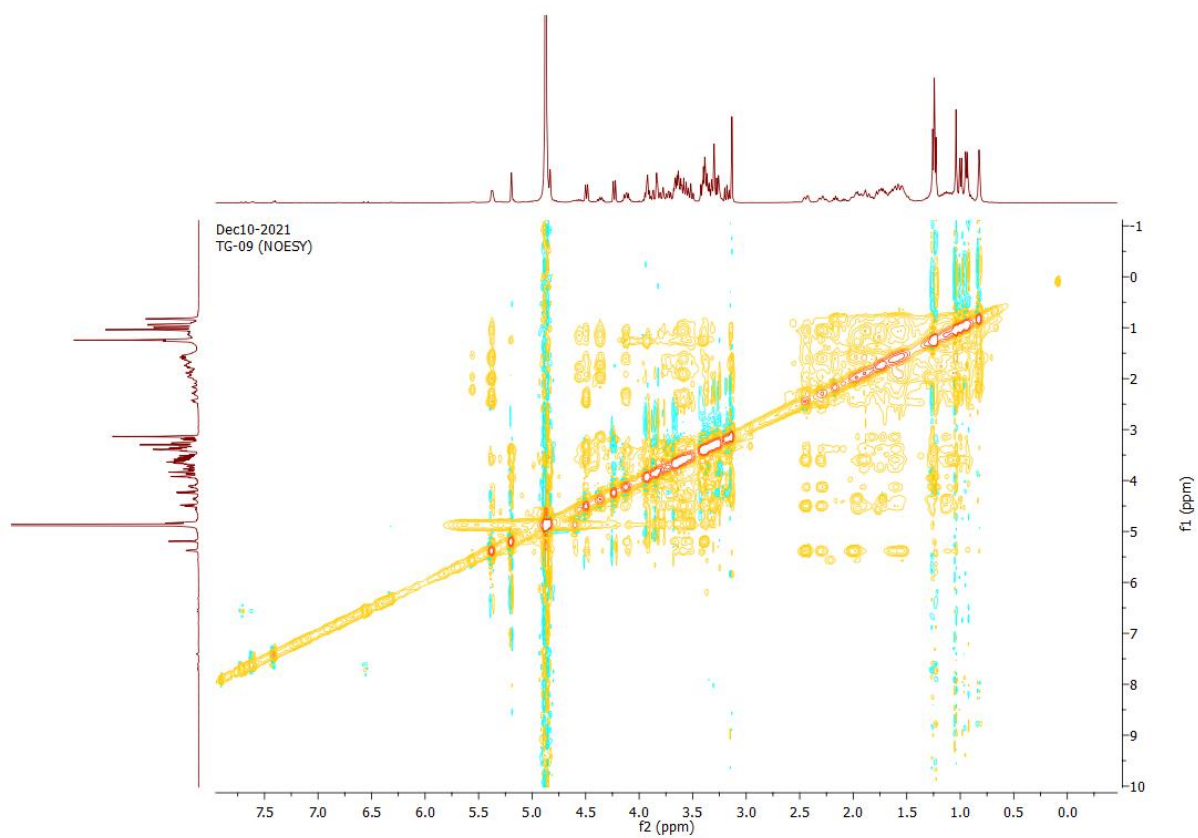


**Figure S16.** NOESY Spectra of compound TG 09

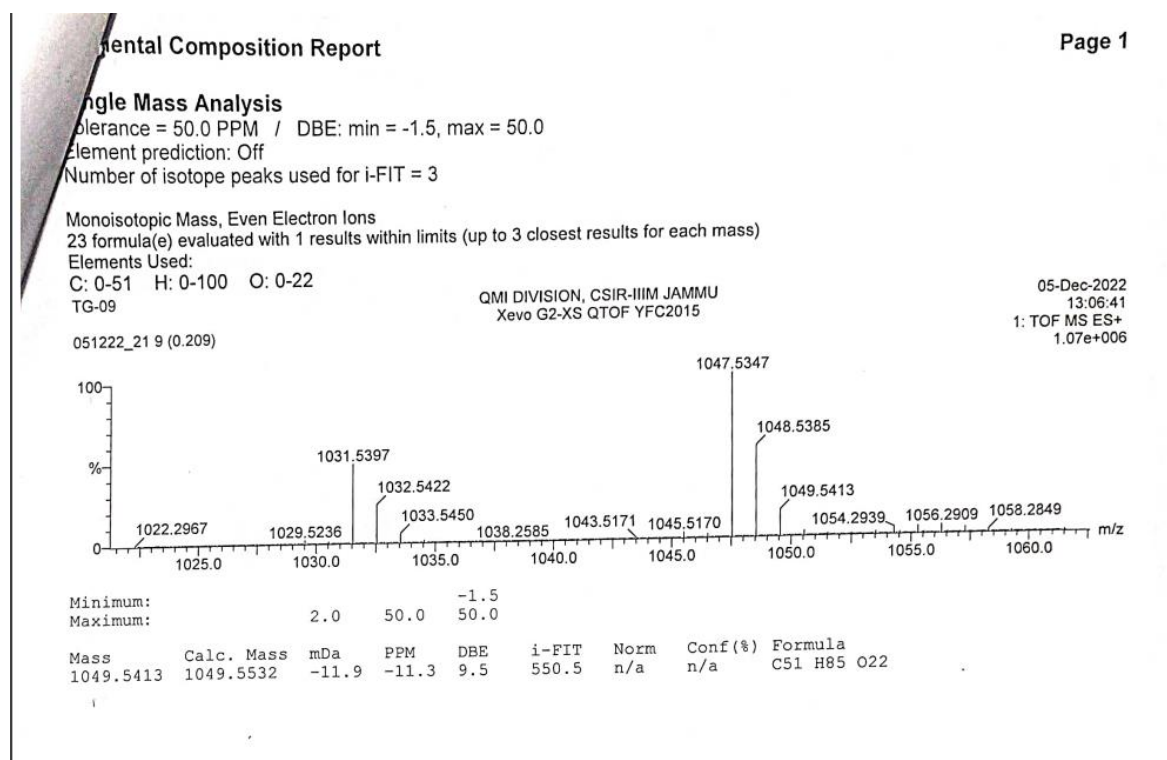
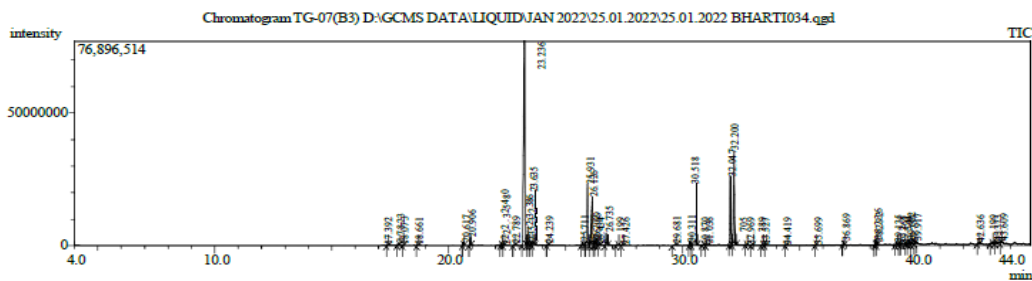


**Figure S17.** HR-ESIMS of compound TG 09

### IIIM GCMS ANALYSIS REPORT

**Sample Information**

Analyzed by : ADMIN  
 Analyzed : 1/26/2022 11:14:29 PM  
 Sample Type : Unknown  
 Sample Name : TG-07(B3)  
 Sample Amount : 1  
 Vial# : 3  
 Injection Volume : 0.50  
 Data File : D:\GCMS DATA\LIQUID\JAN 2022\25.01.2022\25.01.2022 BHARTI034.qgd  
 Method File : D:\GCMS METHOD\GCMS-GENERAL\AMIT 1.qgm  
 Tuning File : D:\Tuning\Tuning-NM-F1 18.01.2022.qgt  
 Modified by : Admin  
 Modified : 1/26/2022 11:59:21 PM



Peak#	R.Time	Area	Area%	Height	Similarity	Peak Report TIC Name
1	23.215	231224721	28.46	76755223	93	Acetyl 2,3,4-tri-O-acetyl-6-deoxy- $\alpha$ -D-glucopyranosid
2	23.635	55669651	6.85	18773884	95	$\alpha$ -L-Talopyranoside, methyl 6-deoxy-, triacetate
3	25.931	84146429	10.36	23296999	95	Methyl 2,3,4-tri-O-acetyl-6-deoxy- $\alpha$ -D-glucopyranosid
4	26.126	63098359	7.77	18205988	93	Acetyl 2,3,4-tri-O-acetyl-6-deoxy- $\beta$ -D-glucopyranoside
5	26.202	4369319	13.54	1550231	88	Tetraacetyl- $\beta$ -L-rhamnose
6	25.530	3965918	0.49	1363282	94	$\alpha$ -D-Xylopyranose, tetraacetate
7	32.047	71127361	18.75	25857099	95	$\beta$ -D-Galactopyranose, pentaacetate
8	32.200	99974618	12.30	35119152	93	$\beta$ -D-Glucopyranose pentaacetate

**Figure S18.** GC/MS analysis of compound TG 07 B3

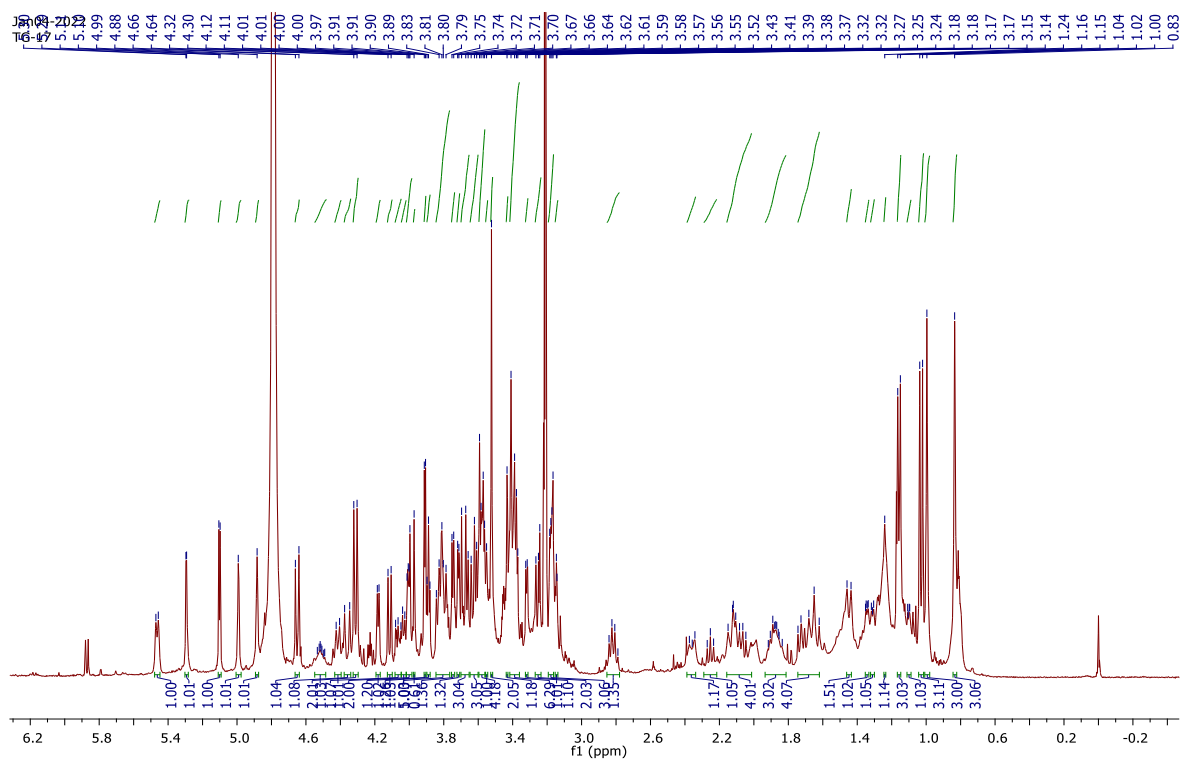


**Figure S19.**  $^1\text{H}$ NMR spectrum of compound **3** (TG-12) ( $\text{CD}_3\text{OD}$ , 500 MHz)

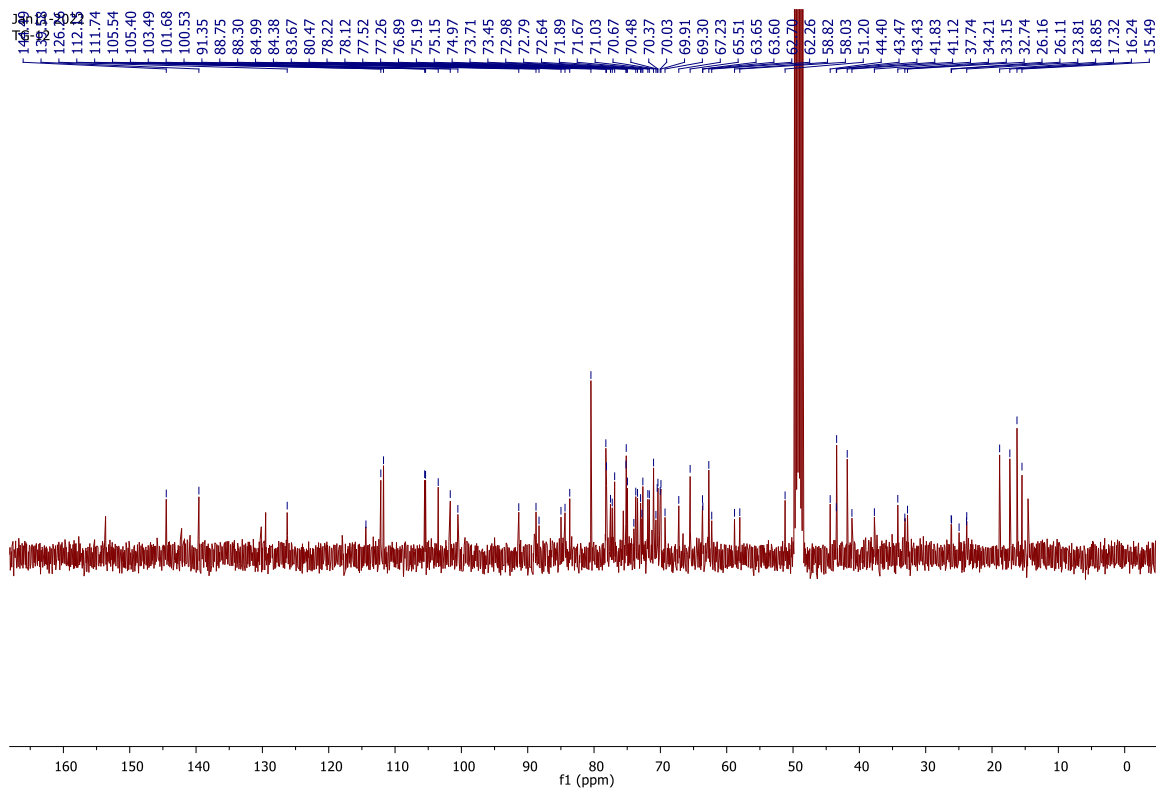


**Figure S20.**  $^{13}\text{C}$  NMR spectrum of compound **3** ( $\text{CD}_3\text{OD}$ , 100 MHz)

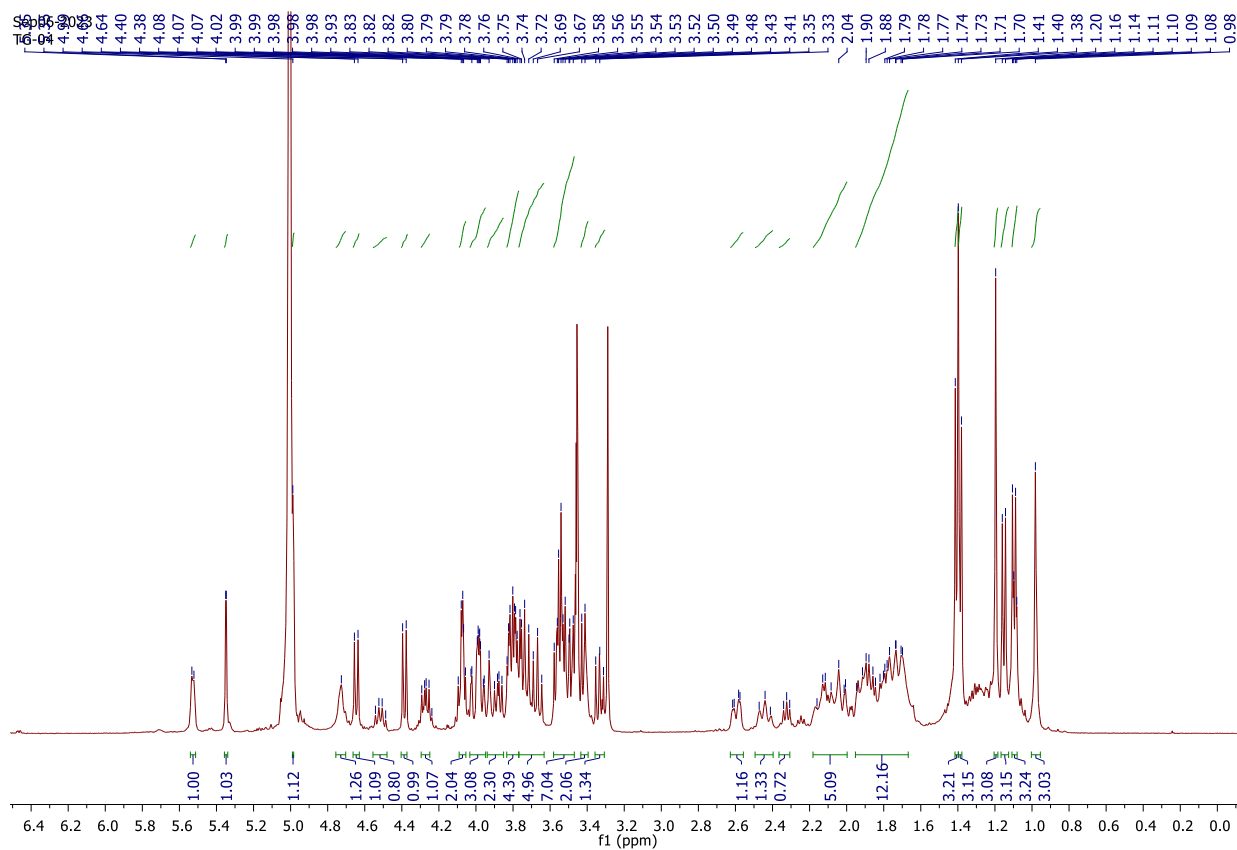


**Figure S21.**  $^1\text{H}$ NMR spectrum of compound **4** (TG-04) ( $\text{CD}_3\text{OD}$ , 500 MHz)

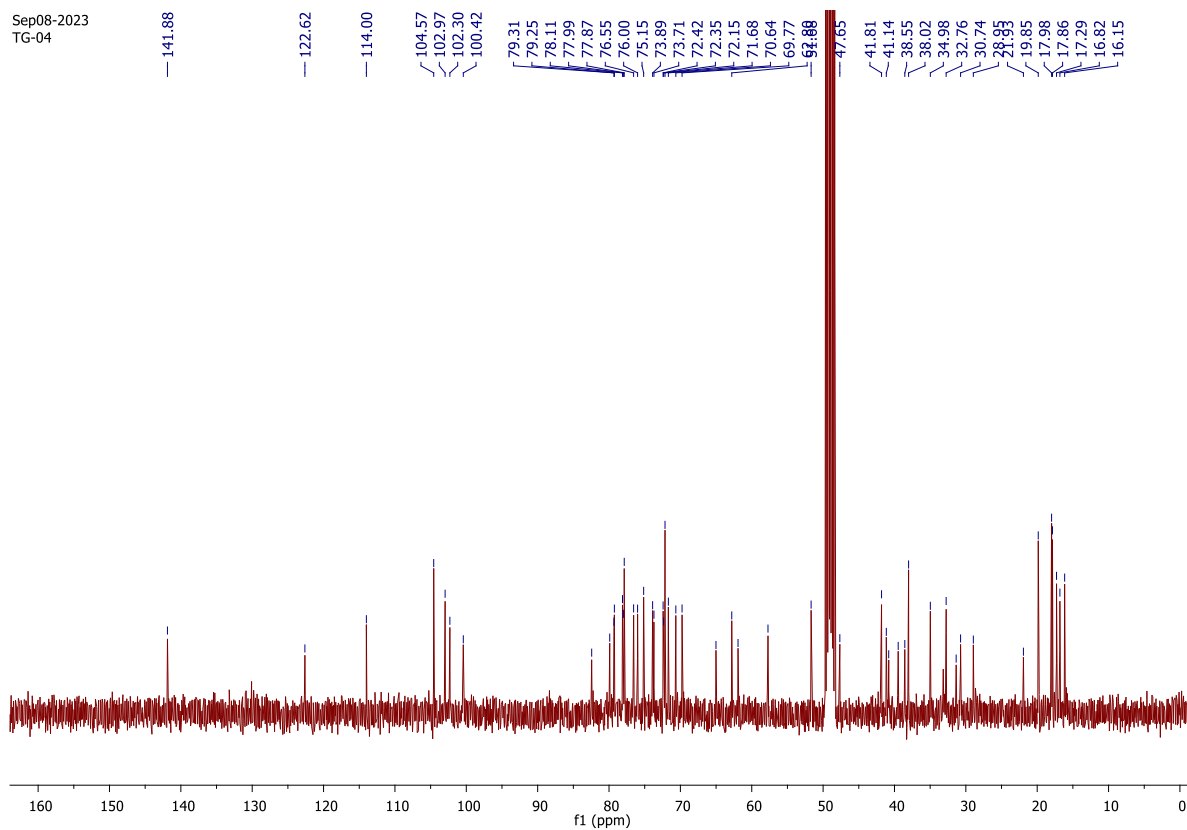


**Figure S22.**  $^{13}\text{C}$  NMR spectrum of compound **4** ( $\text{CD}_3\text{OD}$ , 100 MHz)

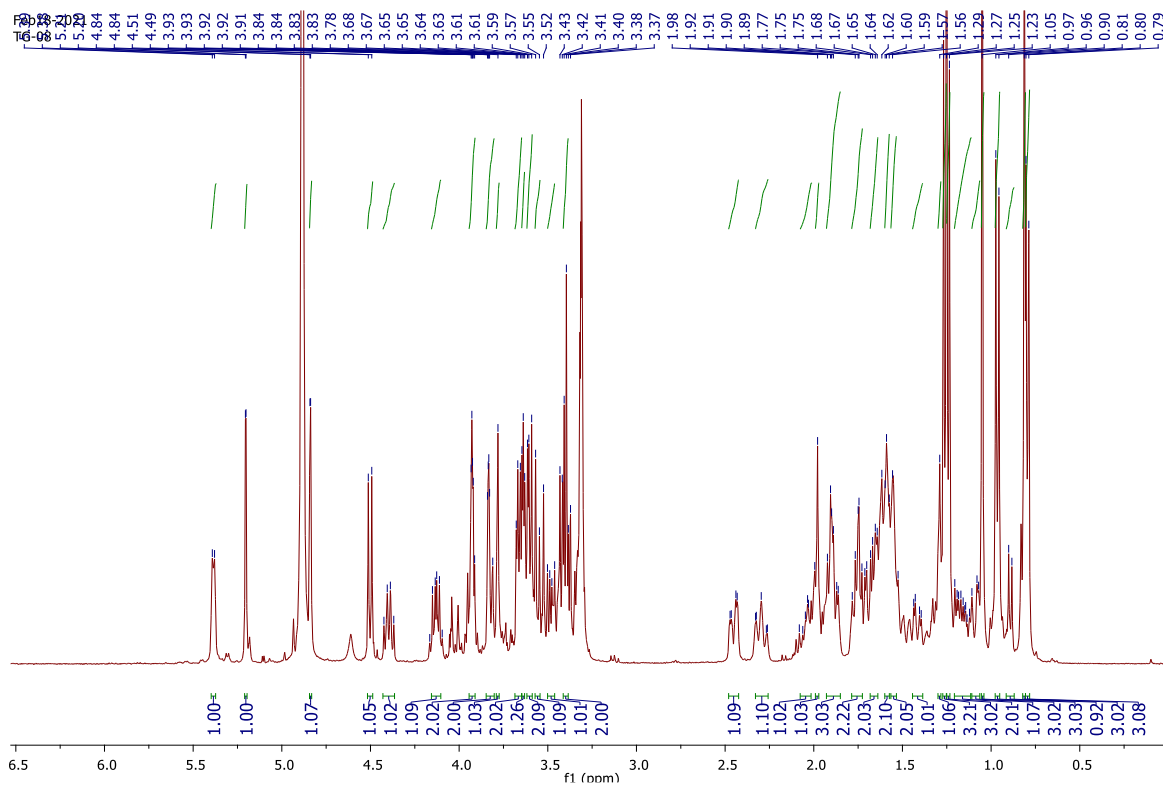


**Figure S23.**  $^1\text{H}$ NMR spectrum of compound **5** (TG-08) ( $\text{CD}_3\text{OD}$ , 500 MHz)

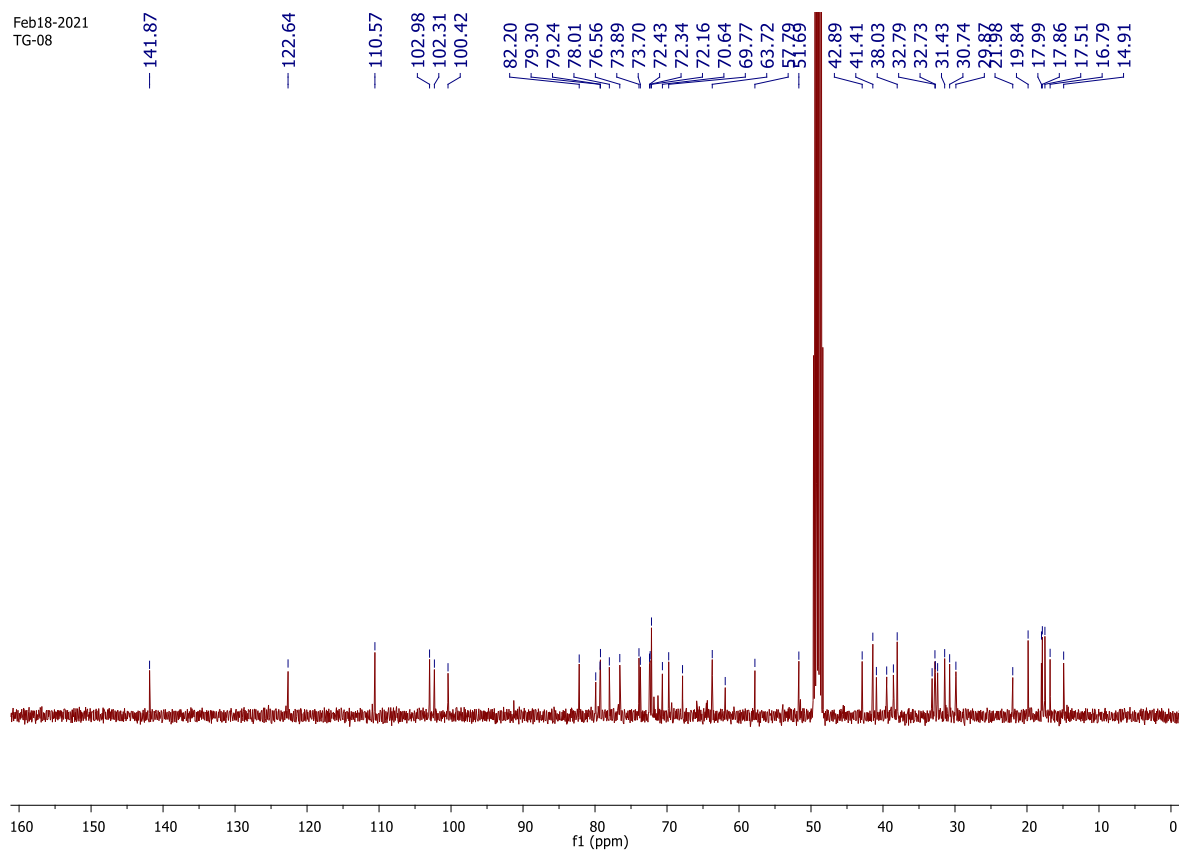


**Figure S24.**  $^{13}\text{C}$  NMR spectrum of compound **5** ( $\text{CD}_3\text{OD}$ , 100 MHz)

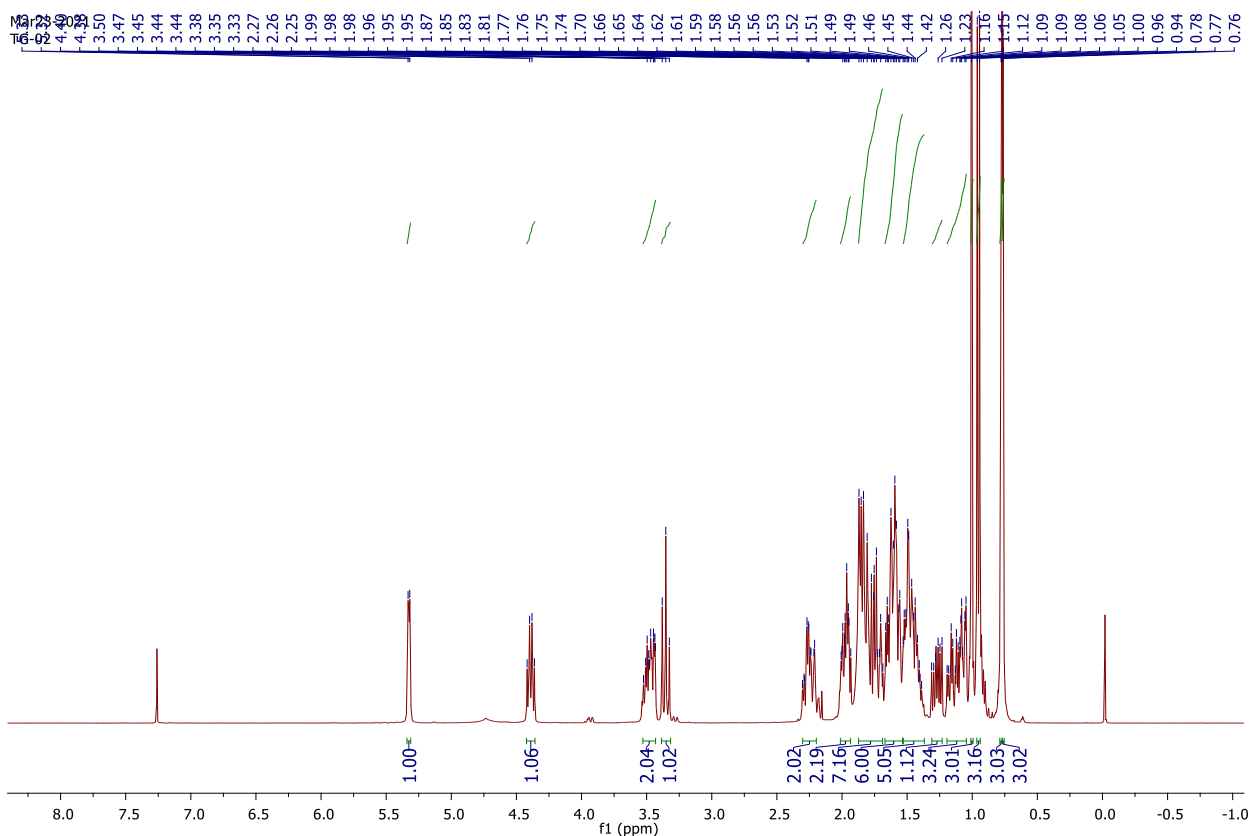


**Figure S25.**  $^1\text{H}$ NMR spectrum of compound **6** (TG-02) ( $\text{CD}_3\text{OD}$ , 500 MHz)

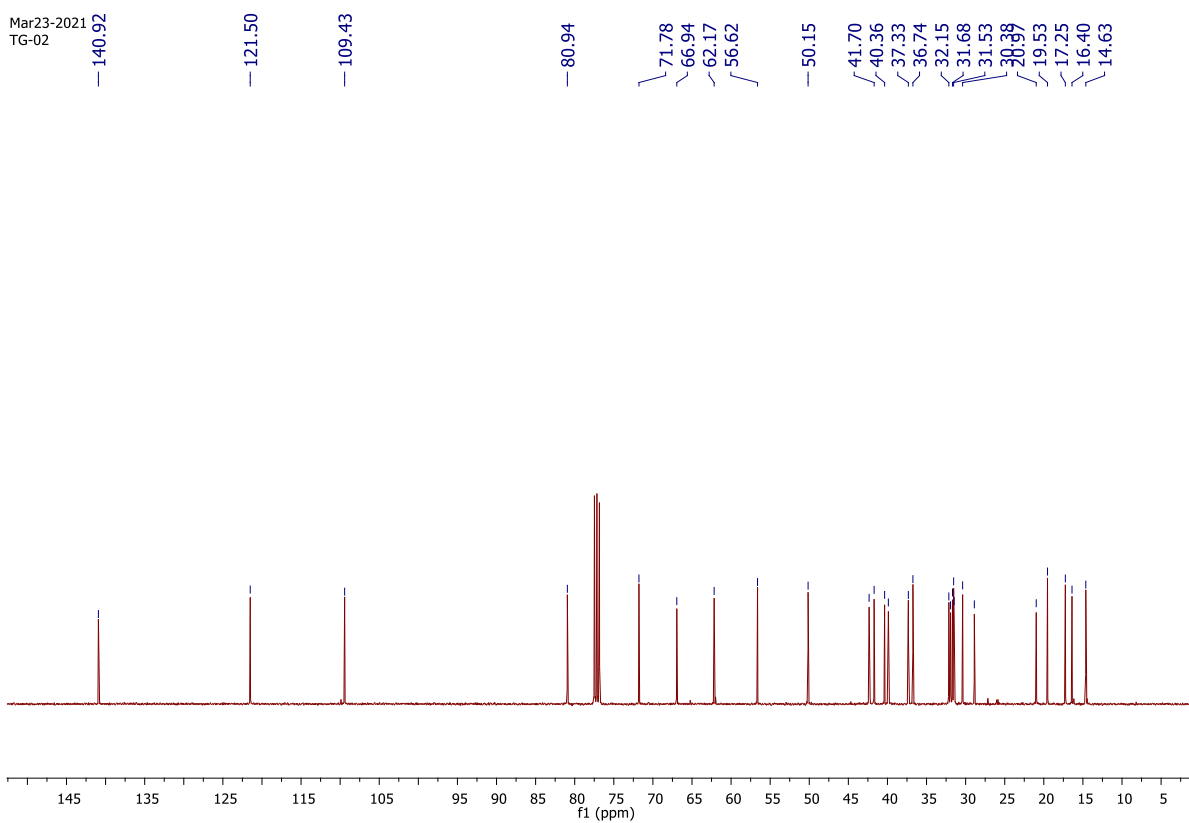


**Figure S26.**  $^{13}\text{C}$  NMR spectrum of compound **6** ( $\text{CD}_3\text{OD}$ , 100 MHz)



Nov10-2020  
TG-01

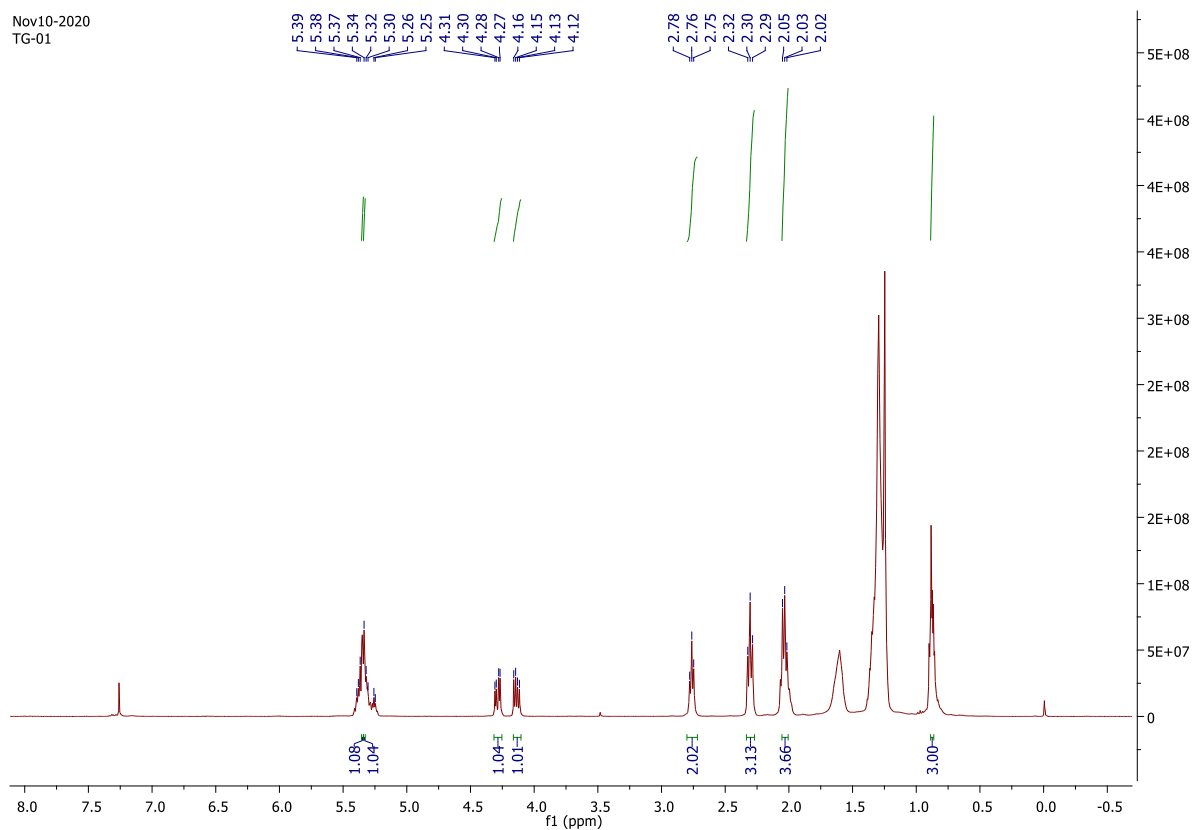


**Figure S27.**  $^1\text{H}$ NMR spectrum of compound **7** (TG-02) ( $\text{CDCl}_3$ , 500 MHz)

Nov10-2020  
TG-01

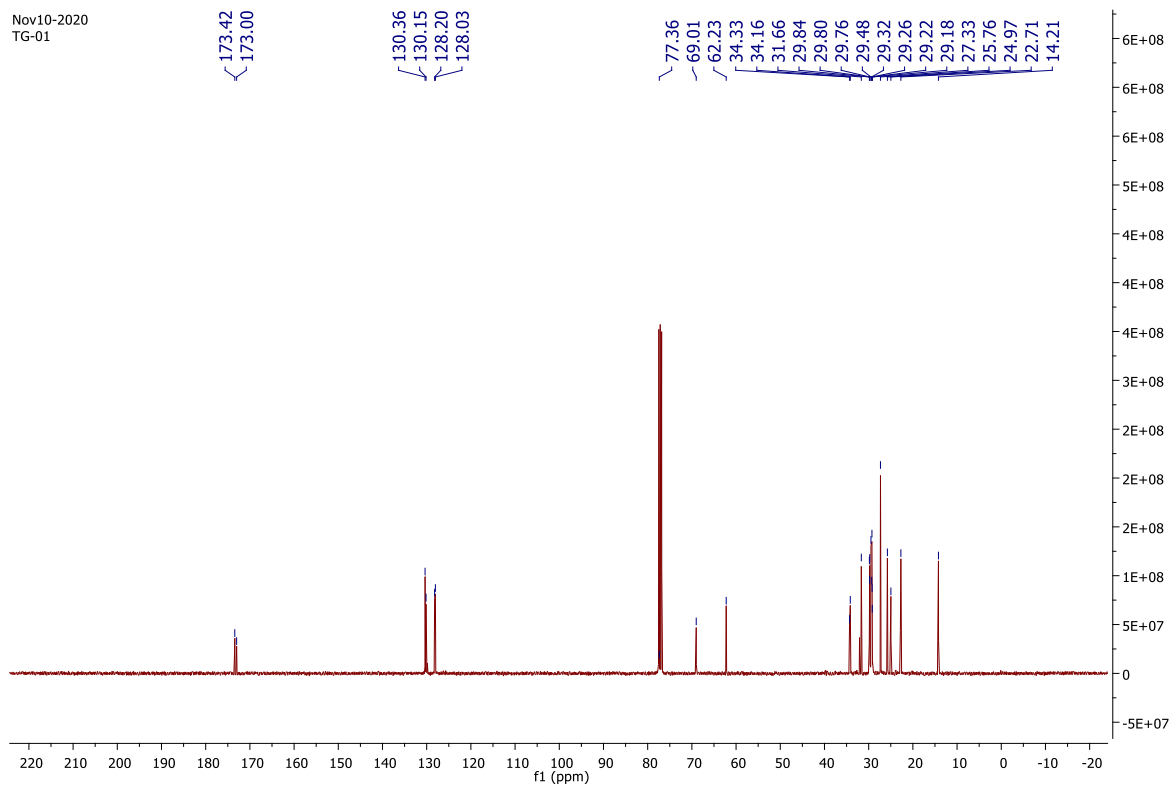


**Figure S28.**  $^{13}\text{C}$  NMR spectrum of compound **7** ( $\text{CDCl}_3$ , 100 MHz)

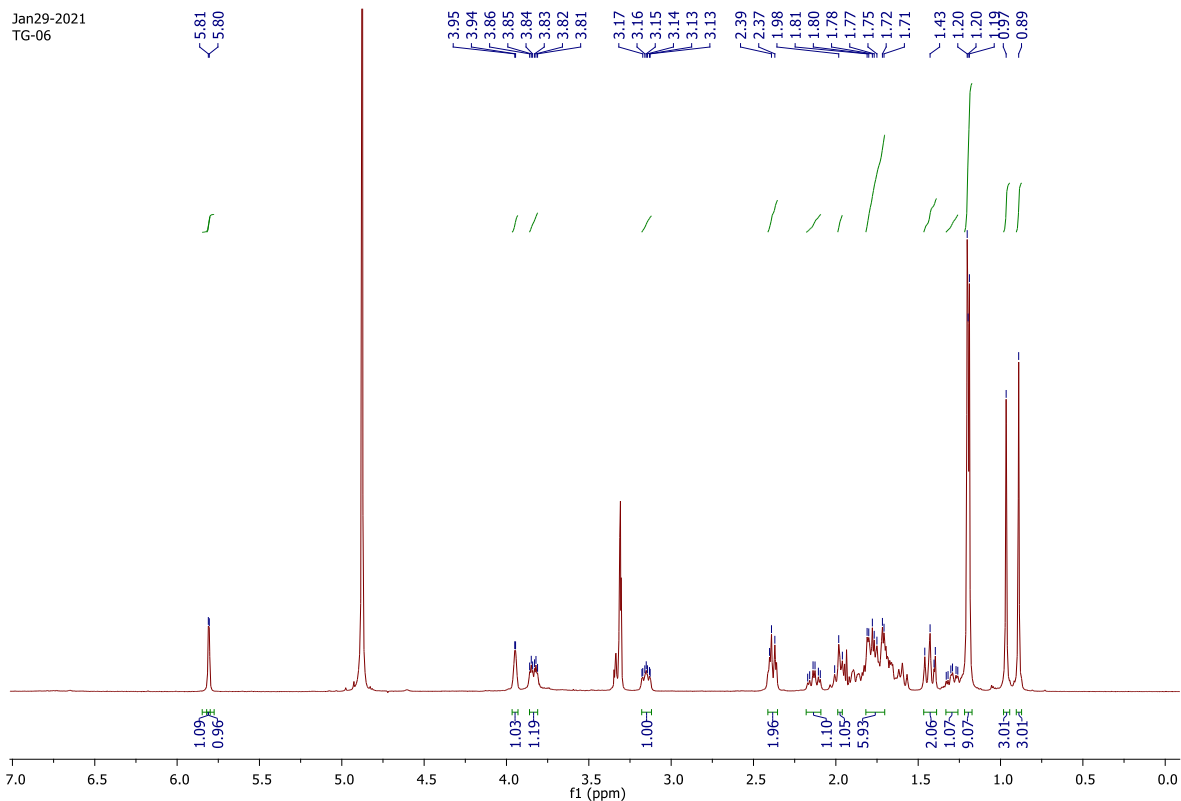


**Figure S29.**  $^1\text{H}$ NMR spectrum of compound **8** (TG-05) ( $\text{CD}_3\text{OD}$ , 500 MHz)

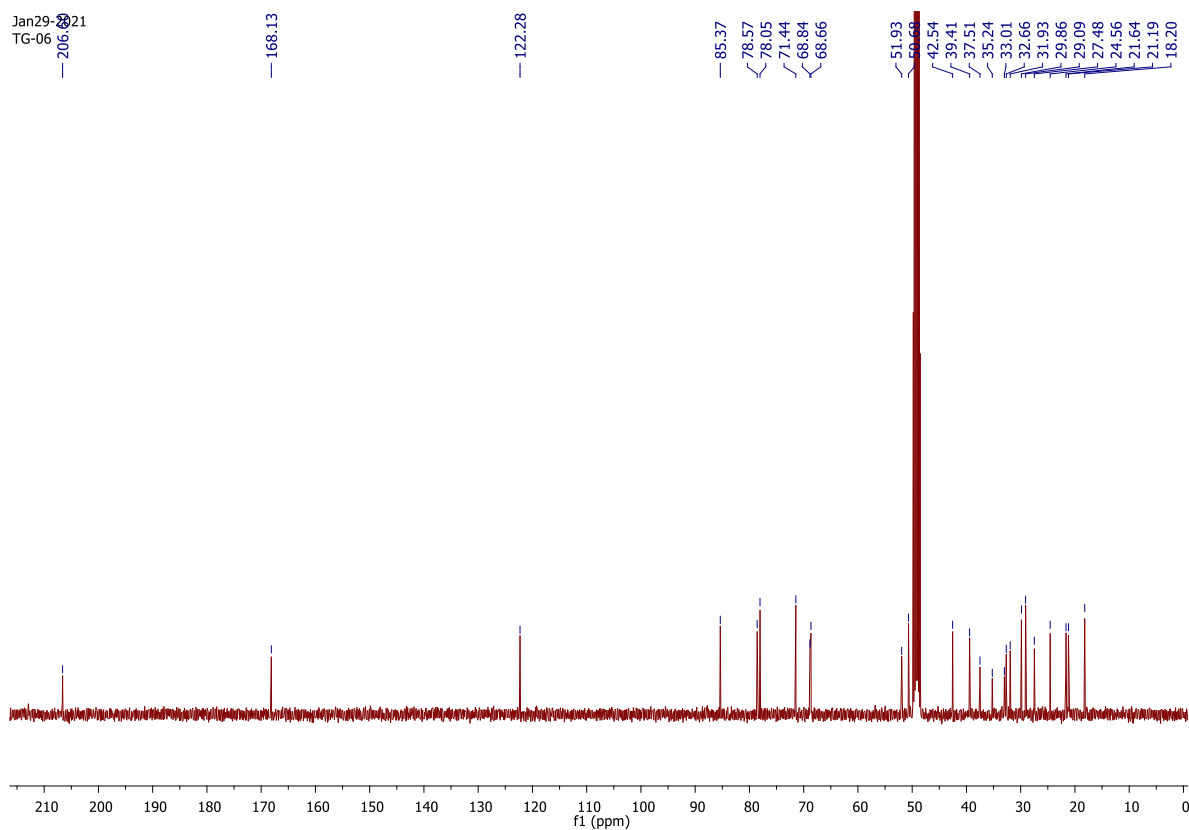


**Figure S30.**  $^{13}\text{C}$  NMR spectrum of compound **8** ( $\text{MeOD}_6$ , 100 MHz)

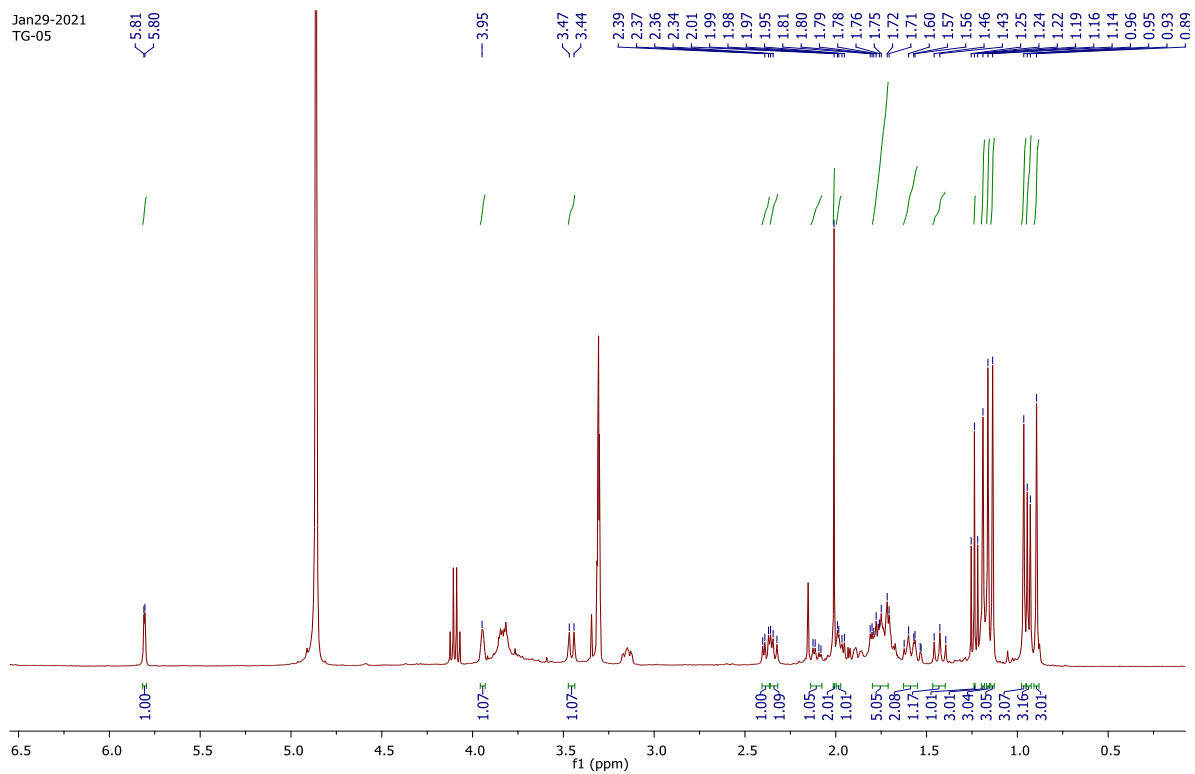


**Figure S31.**  $^1\text{H}$ NMR spectrum of compound **9** (TG-06) ( $\text{CD}_3\text{OD}$ , 500 MHz)

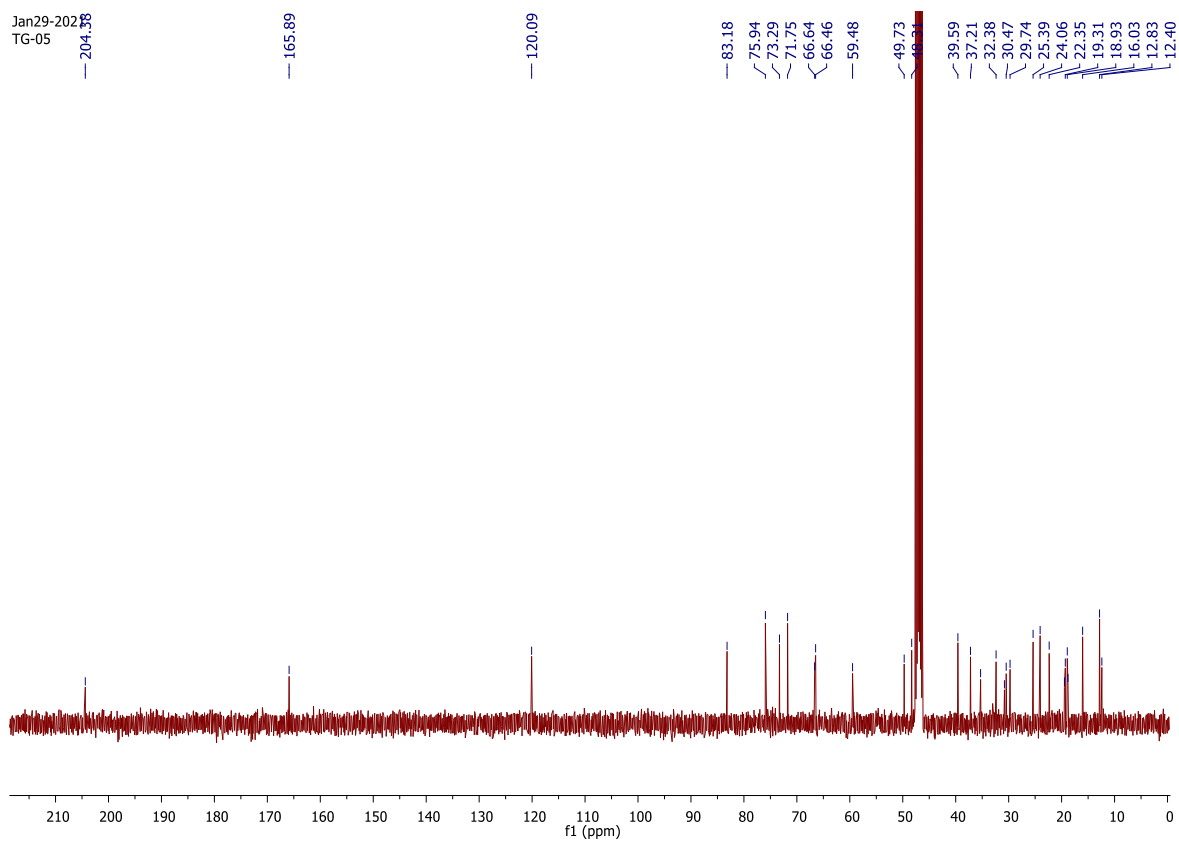


**Figure S32.**  $^{13}\text{C}$  NMR spectrum of compound **9** ( $\text{CD}_3\text{OD}$ , 100 MHz)

**Table 1:** Growth inhibitory effect of Extracts and enriched fractions against different cancer cell lines

Extract & Fractions	Conc. (µg/mL)	Human cancer cell lines						
		Breast	Breast	Colon	Colon	Lung	Pancreatic	Prostate
		MCF-7	MDA-MB-231	HCT-116	SW-620	A-549	MIA PaCa-2	PC-3
		Growth Inhibition (%)						
<b>TG-E1</b>	<b>100</b>	16.88	28.55	11.83	10.97	12.49	<b>ND</b>	<b>ND</b>
	<b>50</b>	5.24	11.87	8.39	3.22	4.56	<b>ND</b>	<b>ND</b>
<b>TG-E3</b>	<b>100</b>	48.22	40.28	72.91	<b>72.50</b>	<b>66.46</b>	30.87	67.75
	<b>50</b>	23.07	18.76	50.73	58.87	35.07	15.74	52.26
<b>TG-EF</b>	<b>100</b>	60.22	58.22	86.66	<b>91.29</b>	<b>96.30</b>	68.87	85.99
	<b>50</b>	45.40	34.78	76.77	75.39	82.78	42.48	66.55

**Table 2:** SRB assay-based screening results. \*\*IC<sub>50</sub> values (μM) of compounds on panel of different human cancer cell lines and normal cell line.

IC <sub>50</sub> (μM)± SD										
Com pd	A- 549	HCT- 116	MCF- 7	MD A- MB 231	Mia PaCa-2	SW- 620	PC-3	SHS Y-5Y	HOP- 62	fR2
1	1.83± 0.54	2.91± 0.50	4.40± 0.33	1.90± 0.26	1.94± 0.24	1.85± 0.52	3.18 ± 0.37	2.43 ± 0.32	1.92± 0.62	13.75 ±0.42
2	1.79± 0.47	3.47± 0.39	5.92± 0.55	9.49± 0.25	-	3.18± 0.40	4.97 ± 0.58	-	-	10.84 ±0.35
3	>50	>50	>50	>50	>50	>50	>50	>50	>50	>50
4	2.08± 0.56	1.95± 0.45	6.98± 0.39	8.29± 0.33	3.79± 0.49	1.98± 0.46	3.77 ± 0.52	3.33 ± 0.26	2.65± 0.47	-
5	1.50± 0.62	4.44± 0.57	4.15± 0.47	2.56± 0.33	1.69 ± 0.45	1.66± 0.38	1.85 ± 0.43	4.43 ± 0.44	1.85± 0.57	2.71± 0.23
6	>50	>50	>50	>50	>50	>50	>50	>50	>50	-
7	30.46 ± 0.49	>50	29.40 ± 0.37	>50	>50	>50	>50	>50	>50	-
8	>50	>50	>50	>50	>50	>50	>50	>50	>50	-
9	32.95 ± 0.43	>50	38.99 ± 0.63	>50	33.26± 0.57	>50	>50	>50	>50	-
<b>CPT</b>	0.030 ±0.04	0.160± 0.23	0.147 ±0.13	0.125 ±0.03	0.060± 0.02	0.093 ±0.03	0.17 0±0. 03	-	0.065 ±0.04	-

## References

1. Sofi, I.I., Verma, S., Charles, B., Ganie, A. H., Sharma, N., & Shah, M. A. 2022. Predicting distribution and range dynamics of *Trillium govanianum* under climate change and growing human footprint for targeted conservation. *Plant Ecology*. 223, 1-17. <https://doi.org/10.1007/s11258-021-01189-3>

2. Ohara, M., Kawano, S., 2005. Life-history monographs of Japanese plants. 2: *Trillium camschatcense* Ker-Gawl (Trilliaceae). Plant Species Biol. 20, 75–82. <https://doi.org/10.1111/j.1442-1984.2005.00126.x>.
3. Chauhan, H.K., Bisht, A.K., Bhatt, I.D., Bhatt, A., Gallacher, D., 2019. *Trillium*-toward sustainable utilization of a biologically distinct genus valued for traditional medicine, Bot. Rev. 85, 252–272. <https://doi.org/10.1007/s12229-019-09211-0>
4. Sharma, P., Samant, S., 2104. Diversity distribution and indigenous uses of medicinal plants in Parbati valley of Kullu district in Himachal Pradesh, North-western Himalaya, Asian. J. Adv. Basic Sci. 2, 77–98. <https://www.jmbm.in/index.php/jmbas/article/view/6>
5. Pant, S., Samant, S.S., 2010. Ethnobotanical observations in the Mornaula reserve forest of Komoun, West Himalaya, India. Ethnobot. Leaflet. 2010,8. <https://opensiuc.lib.siu.edu/ebl/vol2010/iss2/8>
6. Rani, S., Rana, J.C., & Rana, P.K., 2013. Ethnomedicinal plants of Chamba district, Himachal Pradesh, India. J. Med. Plant Res. 7, 3147-3157. [DOI:10.5897/JMPR2013.5249](https://doi.org/10.5897/JMPR2013.5249)
7. Sharma, O.R., Arya, D., Goel, S., Vyas, K., Shinde, P., 2018. *Trillium govaniianum* Wall. ex D. Don (Nagchatri): an important ethnomedicinal plant of Himalayan region (Himachal Pradesh). J. Med. Plants Stud. 6, 11-13. [ISSN \(E\): 2320-3862](https://doi.org/10.2320/3862)
8. Ono, M., Hamada, T., Nohara, T., 1986. An 18-norspirostanol glycoside from *Trillium tschonoskii*. Phytochemistry, 25, 544-545. [https://doi.org/10.1016/S0031-9422\(00\)85524-7](https://doi.org/10.1016/S0031-9422(00)85524-7)
9. Mimaki, Y., Watanabe, K., 2008. Clintoniosides A–C, new polyhydroxylated spirostanol glycosides from the rhizomes of *Clintonia udensis*. Helv. Chim. Acta. 91, 2097-2106. <https://doi.org/10.1002/hlca.200890224>
10. Huang, W., & Zou, K., 2011. Cytotoxicity of a plant steroidal saponin on human lung cancer cells. Asian Pac. J. Cancer Prev, 12(2), 513-517.
11. Ur Rahman, S., Ismail, M., Khurram, M., Ullah, I., Rabbi, F., Iriti, M., 2017. Bioactive steroids and saponins of the genus *Trillium*. Molecules. 22, 2156. <https://doi.org/10.3390/molecules22122156>
12. Yan, T., Wang, A., Hu, G., Jia, J., 2021. Chemical constituents of *Trillium tschonoskii* Maxim. Nat. Prod. Res. 35, 3351-3359. <https://doi.org/10.1080/14786419.2019.1700245>
13. Yan, L.L., Zhang, Y.J., Gao, W.Y., Man, S.L., Wang, Y., 2009. In vitro and in vivo anticancer activity of steroid saponins of *Paris polyphylla* var. *yunnanensis*. Exp. Oncol. 27-32. <http://dSPACE.nbu.gov.ua/handle/123456789/135101>

14. Ya-Zheng, Z.H.A.O., Yuan-Yuan Zhang, H.A.N., Han, F.A.N., Rui-Ping, H.U., Yang, Liang Zhong, K.O.U., Jun-Ping, K.O.U., Bo-Yang, Y.U., 2018. Advances in the antitumor activities and mechanisms of action of steroidal saponins. *Chin. J. Nat. Med.* 16, 732-748. [https://doi.org/10.1016/S1875-5364\(18\)30113-4](https://doi.org/10.1016/S1875-5364(18)30113-4).
15. Ur Rahman, S., Adhikari, A., Ismail, M., Raza Shah, M., Khurram, M., Shahid, M., Ali, F., Haseeb, A., Akbar, F., Iriti, M., 2016. Beneficial effects of *Trillium govanianum* rhizomes in pain and inflammation. *Molecules.* 21, 1095. <https://doi.org/10.3390/molecules21081095>
16. Ismail, M., Shah, M.R., Adhikari, A., Anis, I., Ahmad, M.S., Khurram, M., 2015. Govanoside A, a new steroidal saponin from rhizomes of *Trillium govanianum*. *Steroids*, 104, 270-275. <https://doi.org/10.1016/j.steroids.2015.10.013>
17. Singh, P.P., Suresh, P.S., Bora, P.S., Bhatt, V., Sharma, U., 2021. Govanoside B, a new steroidal saponin from rhizomes of *Trillium govanianum*. *Nat. Prod. Res.* 36, 37-45. <https://doi.org/10.1080/14786419.2020.1761360>
18. Abdel-Sattar, E., Shabana, M.M., El-Mekkawy, S., 2008. Protodioscin and pseudoprotodioscin from *Solanum intrusum*. *Res. J. Phytochem.* 2, 100-105.
19. Yokosuka, A., Mimaki, Y., 2008. Steroidal glycosides from the underground parts of *Trillium erectum* and their cytotoxic activity. *Phytochem.* 69, 2724-2730. <https://doi.org/10.1016/j.phytochem.2008.08.004>
20. Love, J., Simons, C.R., 2020. Acid hydrolysis of saponins extracted in tincture. *PloS one* 15, e0244654. <https://doi.org/10.1371/journal.pone.0244654>
21. Desai, A.G., Qazi, G.N., Ganju, R.K., El-Tamer, M., Singh, J., Saxena, A.K., Bedi, Y.S., Taneja, S.C., Bhat, H.K., 2008. Medicinal plants and cancer chemoprevention. *Curr. Drug Metab.* 9, 581-591. <https://doi.org/10.2174/138920008785821657>
22. Vichai, V., Kirtikara, K., 2006. Sulforhodamine B colorimetric assay for cytotoxicity screening. *Nat. Protoc.* 1, 1112-1116. <https://doi.org/10.1038/nprot.2006.179>
23. Gupta, N., Rath, S.K., Singh, J., Qayum, A., Singh, S., Sangwan, P.L., 2017. Synthesis of novel benzylidene analogues of betulinic acid as potent cytotoxic agents. *Eur. J. Med. Chem.* 135, 517-530. <https://doi.org/10.1016/j.ejmech.2017.04.062>
24. Gupta, N., Sharma, S., Raina, A., Bhushan, S., Malik, F.A., Sangwan, P.L., 2017. Synthesis of Novel Mannich Derivatives of Bakuchiol as Apoptotic Inducer through Caspase Activation and PARP-1 Cleavage in A549 Cells. *ChemistrySelect.* 2, 5196-5201. <https://doi.org/10.1002/slct.201700504>

25. Perillo, B., Di Donato, M., Pezone, A., Di Zazzo, E., Giovannelli, P., Galasso, G., Castoria, G. Migliaccio, A., 2020. ROS in cancer therapy: The bright side of the moon. *Exp. Mol. Med.* 52, 192-203. <https://doi.org/10.1038/s12276-020-0384-2>
26. Ju, Y., Jia, Z.J., 1992. Steroidal saponins from the rhizomes of *Smilax menispermoides*. *Phytochem.* 31, 1349-1351. [https://doi.org/10.1016/0031-9422\(92\)80288-P](https://doi.org/10.1016/0031-9422(92)80288-P)
27. Mimaki, Y., Aoki, T., Jitsuno, M., Kiliç, C.S., Coşkun, M., 2008. Steroidal glycosides from the rhizomes of *Ruscus hypophyllum*. *Phytochem.* 69, 729-737. <https://doi.org/10.1016/j.phytochem.2007.09.022>
28. Braca, A., Prieto, J.M., De Tommasi, N., Tomè, F., Morelli, I., 2004. Furostanol saponins and quercetin glycosides from the leaves of *Helleborus viridis* L. *Phytochem.* 65, 2921-2928. <https://doi.org/10.1016/j.phytochem.2004.07.013>
29. Elmore, S., 2007 Apoptosis: a review of programmed cell death. *Toxicol. Pathol.* 35, 495-516. <https://doi.org/10.1080/01926230701320337>
30. Biancardi, A., Biver, T., Secco, F., Mennucci, B., 2013. An investigation of the photophysical properties of minor groove bound and intercalated DAPI through quantum-mechanical and spectroscopic tools. *Phys. Chem. Chem. Phys.* 15, 4596-4603. <https://doi.org/10.1039/C3CP44058C>
31. Pathania, A.S., Wani, Z.A., Guru, S.K., Kumar, S., Bhushan, S., Korkaya, H., Seals, D.F., Kumar, A., Mondhe, D.M., Ahmed, Z., Chandan, B.K., Malik, F., 2015. The anti-angiogenic and cytotoxic effects of the boswellic acid analog BA145 are potentiated by autophagy inhibitors. *Mol. Cancer.* 14, 1-15. <https://doi.org/10.1186/1476-4598-14-6>
32. Perillo, B., Di Donato, M., Pezone, A., DiZazzo, E., Giovannelli, P., Galasso, G., 2020. ROS in cancer therapy: The bright side of the moon, *Exp. Mol. Med.* 52, 192-203. <https://doi.org/10.1038/s12276-020-0384-2>
33. Gottlieb, E., Armour, S.M., Harris, M.H., Thompson, C.B., 2003. Mitochondrial membrane potential regulates matrix configuration and cytochrome c release during apoptosis. *Cell Death Differ.* 10, 709-717. <https://doi.org/10.1038/sj.cdd.4401231>
34. Kumar, A., Singh, B., Sharma, P.R., Bharate, S.B., Saxena, A.K., Mondhe, D.M., 2016. A novel microtubule depolymerizing colchicine analogue triggers apoptosis and autophagy in HCT-116 colon cancer cells. *Cell Biochem. Funct.* 34, 69-81. <https://doi.org/10.1002/cbf.3166>



35. Rodriguez, L.G., Wu, X., Guan, J.L., 2005. Wound-healing assay. *Cell Migration: Developmental Methods and Protocols*, vol 294. Humana Press. 23-29. <https://doi.org/10.1385/1-59259-860-9:023>
36. Munshi, A., Hobbs, M., Meyn, R.E., 2005. Clonogenic cell survival assay. In: Blumenthal, R.D. (eds) *Chemosensitivity: Methods in Molecular Medicine*, vol 110. Humana Press. 21-28. <https://doi.org/10.1385/1-59259-869-2:021>
37. Majeed, R., Hamid, A., Sangwan, P.L., Chinthakindi, P.K., Koul, S., Rayees, S., Singh, G., Mondhe, D.M., Mintoo, M.J., Singh, S.K., Rath, S.K., Saxena, A.K., 2014. Inhibition of phosphatidylinositol-3 kinase pathway by a novel naphthol derivative of betulinic acid induces cell cycle arrest and apoptosis in cancer cells of different origin. *Cell Death Dis.* 5, e1459-e1459. <https://doi.org/10.1038/cddis.2014.387>